Title

Arginine reprogramming in ADPKD results in arginine-dependent cystogenesis

Journal

American Journal of Physiology. Renal physiology, 315(6)

ISSN

0363-6127

Authors

Trott, Josephine F
Hwang, Vicki J
Ishimaru, Tatsuto
et al.

Publication Date

2018-12-01

DOI

10.1152/ajprenal.00025.2018

Peer reviewed

Arginine reprogramming in ADPKD results in arginine-dependent cystogenesis

Josephine F. Trott[1], Vicki J. Hwang[1], Tatsuto Ishimaru[1], Kenneth Chmiel[1], Xia Zhou[5], Kyuhwan Shim[6], Benjamin Stewart[7], Moe R. Mahjoub[6], Kuang-Yu Jen[3], Dinesh Barupal[2], Xiaogang Li[5] , and Robert H. Weiss[1,4,8]

[1]Division of Nephrology, Dept. of Internal Medicine, [2]West Coast Metabolomics Center, [3]Department of Pathology, and [4]Cancer Center, University of California, Davis, CA, USA, 95616, [5]Kidney Institute, Dept. of Internal Medicine, University of Kansas Medical Center, Kansas City, KS, USA, 66160, [6]Division of Nephrology, Dept. of Medicine, Washington University, St Louis, MO, 63110, [7]Lawrence Livermore National Laboratory, Livermore, CA, USA, 94550, [8]Medical Service, VA Northern California Health Care System, Sacramento, CA, USA, 95655

Running head: Arginine-dependent cystogenesis in ADPKD

CORRESPONDING AUTHOR:
Dr. Robert H. Weiss
Division of Nephrology, Department of Internal Medicine
Genome and Biomedical Sciences Building, Room 6311
451 Health Sciences Dr.
University of California, Davis, CA. 95616

24 e-mail: rhweiss@ucdavis.edu

25 Tel: 530-752-4010; FAX: 530-752-3791

26

ABSTRACT

Research into metabolic reprogramming in cancer has become commonplace, yet this area of research has only recently come of age in nephrology. In light of the parallels between cancer and ADPKD, the latter is currently being studied as a metabolic disease. In clear cell renal cell carcinoma (RCC), which is now considered a metabolic disease, we and others have shown derangements in the enzyme arginosuccinate synthase (ASS1) resulting in RCC cells becoming auxotrophic for arginine and leading to a new therapeutic paradigm involving reducing extracellular arginine. Based on our earlier finding that glutamine pathways are reprogrammed in ARPKD, and given the connection between arginine and glutamine synthetic pathways via citrulline, we investigated the possibility of arginine reprogramming in ADPKD. We now show that, in a remarkable parallel to RCC, ASS1 expression is reduced in murine and human ADPKD, and arginine depletion results in a dose dependent compensatory increase in ASS1 levels as well as decreased cystogenesis *in vitro* and *ex vivo* with minimal toxicity to normal cells. Non-targeted metabolomics analysis of mouse kidney cell lines grown in arginine-deficient vs. arginine-replete media suggests arginine-dependent alterations in the glutamine and proline pathways. Thus, depletion of this conditionally-essential amino acid by dietary or pharmacological means, such as with arginine-degrading enzymes, may be a novel treatment for this disease.

INTRODUCTION

Research into metabolic reprogramming has been fruitful in cancer for several years and is on the cusp of yielding both a greater understanding of, and new therapeutic approaches for, polycystic kidney disease (PKD). While, unlike cancer, ADPKD cells have little need to evade immune surveillance, they do, like malignancy, need to synthesize biochemical and membrane components to enable relatively rapid growth and consequent cyst expansion. Previous studies from our and other laboratories have demonstrated reprogramming of glutamine in autosomal recessive PKD (ARPKD)(16) and glucose in autosomal dominant PKD (ADPKD)(38) models.

In humans, arginine is a “conditionally” essential amino acid, being required only at specific times in organismal development. However, renal cell carcinoma (RCC) tissues(34, 46) and cells(49) demonstrate remarkably decreased levels of the arginine synthetic enzyme ASS1 resulting in these tumors being auxotrophic for arginine both *in vitro* and *in vivo* in the RENCA model of RCC(49). In light of the fact that ADPKD exhibits differential behavior depending on developmental stage(35) and given the known parallels of ADPKD with RCC, we asked whether ADPKD shows arginine reprogramming in a similar manner to what is observed in cancer. We now demonstrate that arginine, although a non-essential amino acid, regulates ASS1 levels and is required for cystogenesis in PKD cells and in an ex vivo cystogenesis model; thus arginine reductive therapies may be useful in cystic disease with minimal toxicities to normal adult tissues.

METHODS

Tissues and cells

Mouse postnatal *Pkd1*-heterozygous (PH2) and *Pkd1*-homozygous null (PN24) cells were of proximal tubule origin and cultured as described(41) (provided by S. Somlo through the George M O'Brien Kidney Center, Yale University, New Haven, Connecticut, USA). The genotype of these cells was validated and confirmed by PCR to detect the Neo cassette inserted into exon 1 of the null allele (in both PH2 and PN24 cells) using primers in exon 1 (E1F5 CCCTCCTGAACTGCGGCT and E1R5 CAGGGTCTCCGGCCAGCG) and a Neo cassette specific primer set (NEOF3 AGCGCATCGCCTTCTATCGC and E1R5). They were also checked for the Cre-lox excision of exons 2-4 on the floxed allele (PN24 cells only) with primers in intron 1 (LoxF1 CCGCTGTGTCTCAGTGCCTG and LoxR1 CAAGAGGGCTTTTCTTGCTG) and primers spanning intron 1 and exon 5 (D1L1FY CAGCCTGCCTTGCTCTACTT and D1E5R3 TCACCAGCTGAGAAGCAGAA). Mouse embryonic kidney (MEK) *Pkd1*-null and MEK WT cells were of collecting duct origin and cultured as previously described(54). The excision of exons 3-4 from both alleles of the PKD-1 gene from MEK Pkd1-null cells was validated and confirmed by PCR (mPKD-1ex4 F GCTGGGCAAAGGAACATCAG and mPKD-1ex6 R GACATTGCTCCTGTGCTTGC; mPKD-1ex1 F GGGCCCCTCCTGAACTGC and mPKD-1ex4 R GTTGCACTCAAATGGGTTCC). Mouse experiments as described previously (17) were performed under appropriate IACUC approvals. *Pkd1*$^{+/+}$*:Pkhd1-Cre, Pkd1*$^{+/flox}$*:Pkhd1-Cre* and *Pkd1*$^{flox/flox}$*:Pkhd1-Cre*(17) male and female mouse kidneys were dissected out at post-natal day 5 (P5), P10, P14, P21 and P25 and either snap frozen for immunoblotting and/or qPCR or fixed in 4% paraformaldehyde and paraffin embedded

for immunohistochemistry. Human ADPKD and NHK tissues used for immunoblotting and qPCR, and ADPKD kidneys for immunohistochemistry, were obtained from Dr. Darren Wallace (Kidney Institute, Departments of Internal Medicine and Physiology, University of Kansas Medical Center). Normal human kidneys for immunohistochemistry were archived following IRB approval at the UC Davis Department of Pathology.

Cell Culture

MEK WT and MEK *Pkd1*-null cells were cultured at 37^{o}C in MEK media (DMEM/F-12, 2% FBS, ITS (15 µg/ml; GenDepot), 3,3′,5-Triiodo-L-thyronine (100 nM; Sigma-Aldrich), hydrocortisone (36 ng/ml; Sigma-Aldrich), mouse IFNγ (5U/ml), penicillin and streptomycin(30). PH2 and PN24 cells were cultured at 37^{o}C in PHPN media (DMEM/F-12, 10% FBS, mouse IFNγ (5U/ml), penicillin and streptomycin). Arginine defined media was MEK media prepared with arginine, lysine and glutamine free DMEM/F-12 (Caisson Laboratories Inc), supplemented with 0.5 mM lysine (Sigma-Aldrich), 2.5 mM GlutaMAX (ThermoFisher) and various concentrations of L-arginine monohydrochloride (Sigma-Aldrich). The concentration of arginine in the lot of FBS used for all experiments was measured to be 3.38 µM so the actual concentration of arginine in our 0 mM arginine MEK media was 0.07 µM.

In Vitro Proliferation Assays

Cells ($1.5x10^3$ or $3x10^3$) were plated in 96-well plates and after the cells had attached, were treated with MEK media containing 0-0.7 mM arginine for 3 or 5 days. Media was changed either at 36 h (3 day assay) or at 48 and 96 h (5 day assay). Cells

were stained either with Thiazolyl Blue Tetrazolium Bromide (MTT) as previously described(17) or with methylene blue as previously described(5).

In Vitro Cyst Assays

For cyst assays PH2, PN24, MEK WT and MEK *Pkd1-null* cells were cultured at 37^{o}C for 7-14 days in MEK media without mouse IFNγ then plated in 96 well plates (2000 cells/well) in 66% Corning™ Matrigel™ Membrane Matrix (Fisher Scientific, Pittsburg, PA), overlaid with MEK media without mouse IFNγ containing various concentrations of arginine. The media was changed daily, and cysts were photographed and diameters measured on days 13 or 14 after plating.

Western blotting

Immunoblotting was performed as previously described (16). The antibodies used were monoclonal (2B10) mouse anti-ASS1 antibody (Invitrogen, Carlsbad, CA), rabbit anti-vinculin (Cell Signaling Technology, Danvers, MA) and rabbit anti-β-actin (Cell Signaling Technology). Signal was detected with ECL using a FujiFilm LAS-4000 or x-ray film and Image J to quantify band intensity.

Immunohistochemistry

Paraffin sections (4 μm) of formalin-fixed paraffin-embedded (FFPE) human kidneys were stained for ASS1 as described(34) with the following modifications: monoclonal anti-human ASS1 antibody clone 2B10 (Invitrogen) diluted in PBST was followed by MACH2 Universal HRP-Polymer (BioCare Medical) and ImmPACT

diaminobenzidine peroxidase substrate (Vector Laboratories, Burlingame, CA). Paraffin sections (4 µm) of FFPE mouse kidneys were stained for ASS1 using monoclonal anti-human ASS1 clone 2B10 (Invitrogen) with the Mouse on Mouse HRP-polymer bundle (BioCare Medical, Concord, CA) and ImmPACT diaminobenzidine peroxidase substrate (Vector Laboratories, Burlingame, CA).

RNA extraction, reverse transcription and qPCR

RNA extraction, reverse transcription of mRNA into cDNA, primer design and qPCR were all performed as previously described(45) with the following modifications: in addition to *Rn18S,* two new housekeeping genes (*Eef2* and *Rpl13a*) were chosen for normalization of mouse *Ass1* mRNA based on multiple instances identifying them as excellent housekeeping genes(6, 7, 21) (Supplemental Table 1). Standard curves for qPCR were prepared using 6 or 7 five-fold dilutions of human or mouse normal kidney cDNA. All standard curves had a linear regression coefficient of determination of at least 99%. The mRNA or rRNA levels of each gene in each mouse or human sample were calculated using a relative standard curve of cDNA quantity plotted against Ct. Normalization of gene expression relative to three housekeeping (reference) genes was completed according to the formula:

$$Y_i = \frac{Q_{Ti}}{\sqrt[3]{Q_{R1i} x Q_{R2i} x Q_{R3i}}}$$

where Y is the normalized *hASS1* or *mAss1* gene expression for tissue/cell line i, Q_{Ti} is *hASS1* or *mAss1* mRNA quantity and Q_{R1i}, Q_{R2i} and Q_{R3i} are reference gene quantities.

Bisulfite gDNA modification and methylation specific PCR

gDNA was extracted from tissue samples and cell lines using the DNAeasy Tissue Kit (Qiagen). The EZ DNA Methylation Kit (Zymo Research Corporation, Irvine, CA) was used on 500 ng purified gDNA to convert unmethylated cytosine residues to uracil while not affecting methylated cytosines. Methylation-specific PCR (MSP) of the *hASS1* gene was performed as previously described(27) using primers in Supplemental Table 2. MethPrimer(24) was used both to find a CpG island in the mouse ASS1 promoter, 328-59 bp upstream of the transcription start site (TSS), and to design primers for MSP of this region. MSP was performed on a 102-104 bp fragment of the *mAss1* gene located 315-213 bp upstream of the TSS. All MSP reactions were performed using EpiMark Hot Start Taq Polymerase (New England Biolabs, Ipswich, MA) on 1 µl of bisulfite-modified DNA with 200 nM of primers specific for methylated (M) or unmethylated (U) sequences. PCR reactions were heated to 95^{o}C for 30s, then 40 cycles of 95^{o}C 15 s, annealing for 1 min (*hASS1*) or 1.5 min (*mAss1*) and 68^{o}C for 30 s, followed by a final extension of 68^{o}C for 5 min. PCR products were run on 2% agarose gels and visualized using ethidium bromide. Cancer cells (human 786-O and mouse RENCA) were used as positive controls for methylated gDNA, non-bisulfite gDNA was used as a negative control.

Non-targeted metabolomics analysis

Non-targeted metabolomics on cell lysates was accomplished by the West Coast Metabolomics Center at UC Davis as previously described(8, 43).

Targeted metabolite analysis

Media from cultured cells was collected and diluted to give a ratio of 1:1:4 (Media: 50% methanol in water: Acetonitrile with 0.15% formic acid). Arginine and glutamate were separated on a Waters Acquity H Class HPLC system and measured with a Waters Xevo G2-XS QTOF instrument (Waters Corporation, Milford, MA USA). For chromatographic separations, the HPLC method reported by Guo et al(13) was used with minor modifications as follows: acetonitrile with 0.15% formic acid was used as the organic mobile phase (B), and the gradient was initial, 85%B; 6 min, 80% B; 10 min, 55% B; 12.5 min, 45% B, 12,6 min, 5% B, 14 min, 5% B, 14.1 min, 85% B, 18 min, 85% B. The column was a Waters Acquity BEH Amide 1.7 µm, 2.1 x 150 mm column, the flow rate was 0.4 mL/min, and the run time was 18 minutes. Metabolite standards were prepared in concentrations from 1-400 µM in 50% Acetonitrile/50% 10 mM ammonium formate + 0.15% formic acid for quantitation. Detection was accomplished in positive electrospray, centroid MS^e data acquisition mode over m/z range of 50-1000. Low energy collision voltage was 6 V and high energy voltage ramped from 10 to 40 V. Lockmass correction was applied using leucine enkephalin. Data acquisition was accomplished using MassLynx 4.1 software, and data analysis was performed with TargetLynx software (Waters Corporation).

Arginine levels in FBS were measured on a Thermo Surveyor HPLC System attached to a Thermo Orbitrap mass spectrometer. The separation was performed on a Waters Atlantis T3 4.6 x 250 mm column. The mobile phase consisted of 75% water with 0.1% formic acid and 25% acetonitrile. Flow was isocratic at a rate of 1 mL/minute and analysis time was 3.5 minutes. The column thermostat was held at 70° C. Injection volume was 2 µL. Electrospray ionization in positive mode was used to scan ions from

100 to 500 m/z. Quantitation was performed using external standards and analysis with Thermo Xcalibur Quant Browser software. Samples and calibrants were measured in triplicate.

Ex vivo kidney organ cultures

Ex vivo cystogenesis assays were performed as previously described(2, 16, 26). Briefly, metanephroi were dissected from embryonic CD1 mice at embryonic day 13.5 and placed on transparent Transwell cell culture inserts (Corning). DMEM/F12-defined culture medium (supplemented with 2 mml/l L-glutamine, 15 mmol/l N-2-hydroxyethylpiperazine-N0-2-ethanesulfonic acid, 5 mg/ml transferrin, 10 mmol/l sodium selenite and 10 mmol/l prostaglandin E1; all from Sigma-Aldrich) was added to the basal chamber, and organ cultures were maintained in a 37^{o}C humidified CO_2 incubator for up to 5 days. To induce cystogenesis, the culture medium was supplemented with 100 µmol/l 8-bromoadenosine 30,50-cyclic monophosphate (8-Br-cAMP; Sigma-Aldrich) and culture media containing either 0.25 mg/ml, 0.12 mg/ml or 0.06 mg/ml arginine was changed daily. Kidneys were imaged every 24 hours for 5 days using a 2x or 4x objective. Quantification of cystic number and area was performed using NIS-Elements AR 4.20 software (Nikon). Four kidneys were analyzed per experimental sample.

RESULTS

Since an early indication of arginine reprogramming and auxotrophy in kidney cancer was gleaned from the observation that ASS1 levels were decreased in RCC tumors, we first evaluated protein and mRNA levels of this enzyme in mouse models of

ADPKD as well as in tissues from ADPKD affected individuals. The mouse embryonic kidney cell line MEK-wt and its *Pkd1*-null counterpart MEK-null(54), as well as the *Pkd1* heterozygous postnatal kidney cell line PH2 and its homozygous *Pkd1*-null counterpart PN24(41), both showed markedly decreased levels of ASS1 protein and mRNA in the *Pkd1*-null cells as compared to the wild-type cells (Fig. 1a). We also quantitated ASS1 protein and mRNA levels in the well-established early-stage ADPKD mouse model *Pkd1*$^{flox/flox}$*:Pkhd1-Cre* compared to *Pkd1*$^{+/+}$*:Pkhd1-Cre* mouse kidneys(17, 54) and found a similar phenomenon (Fig. 1b). Furthermore, quantification of ASS1 protein and mRNA levels in human nephrectomy tissues from six individuals with ADPKD and three normal individuals showed results (Fig. 1c) consistent with the mouse data.

We further investigated both the timing of when ASS1 expression starts to decrease in kidneys with ADPKD and also which cell types within the kidneys are expressing ASS1. In normal human kidneys, the expression of ASS1 is diffusely strong in the proximal tubules and slightly less in the parietal epithelial cells of the Bowman capsule (Figs 2A-D). Interestingly, in the ADPKD tissues, the staining intensity of ASS1 is similar to that in normal kidneys in the non-atrophic proximal tubules, however there is a large amount of interstitial fibrosis and tubular atrophy, with diminished or loss of ASS1 protein expression in atrophic tubules (Figs 2E-J). Remnant non-atrophic proximal tubules showing retained strongly positive ASS1 expression is evident in patients ADPKD 393A (Fig. 2E) and ADPKD 374 (Fig. 2I) but the other cysts and atrophic tubules are lined by cells that generally exhibit weaker, minimal, or absent ASS1 expression (Figs 2G, H and J).

253 We further examined which cells are expressing ASS1 in mouse kidneys using
254 immunohistochemical stains (Fig. 3). Similar to human kidneys, in mice there is
255 substantial murine Ass1 (mAss1) staining in proximal epithelial cells and minimal mAss1
256 staining in distal tubule and glomerular cells from P5 kidneys of wild-type mice as well
257 as mice either heterozygous or homozygous for Pkd1 mutation (Figs. 2 and 3). In
258 contrast to the human kidney, there was minimal mAss1 expression in the parietal
259 epithelium of the Bowman capsule (Fig. 3). Whereas in the human the cystic epithelium
260 is generally stained with ASS1, in mice, at P14 and 21 after cysts have developed, the
261 cystic epithelium is variably stained for mAss1, but substantial fibrosis is present in both
262 species (Figs. 2 and 3). Using immunoblotting to quantify the expression of mAss1 in
263 *Pkd1*$^{+/+}$*:Pkhd1-Cre* vs *Pkd1*$^{+/flox}$*:Pkhd1-Cre* vs *Pkd1*$^{flox/flox}$*:Pkhd1-Cre* mouse kidneys, we
264 found mAss1 did not differ at postnatal day 10 (P10) or P14 (Fig. 4). However by P21
265 there was a significant loss of mAss1 in *Pkd1*$^{flox/flox}$*:Pkhd1-Cre* mouse kidneys compared
266 to *Pkd1*$^{+/+}$*:Pkhd1-Cre* and *Pkd1*$^{+/flox}$*:Pkhd1-Cre* ($p<0.002$; Fig. 4).
267 In cancer cells that are treated with arginine deprivation, resistance develops as
268 the cells increase their expression of ASS1 protein(25). We next asked whether a
269 similar phenomenon occurs in vitro in the two ADPKD cell lines used in this study and
270 their normal cell line counterparts. PN24 cells grown in the presence of several
271 concentrations of media arginine (0.7, 0.1 or 0 mM) for 1 week did not show a
272 significant change in *ASS1* mRNA (data not shown). However, with 2 weeks of growth
273 in the presence of 0.7, 0.1 or 0.001 mM (MEK) or 0 mM (PN24) arginine, both MEK
274 *Pkd1*-null and PN24 cells demonstrated an arginine dose-dependent increase in ASS1
275 protein and mRNA (Fig. 5a) suggesting a compensatory response of arginine synthesis

when the cells are unable to obtain sufficient arginine from the media. By contrast, the *Pkd1* +/+ (MEK WT) cell line does not significantly increase ASS1 protein or mRNA expression after 2 weeks' growth in the presence of 0.001 vs 0.7 mM arginine (Fig. 5b). While the *Pkd1* +/- (PH2) cell line did increase ASS1 protein expression after 2 weeks of culturing in 0 mM vs 0.7 mM arginine this increase was not consistent with the ASS1 mRNA levels (Fig. 5b).

In RCC and other cancers, ASS1 regulation occurs via epigenetic promotor methylation(15, 22), and for this reason we asked whether the same mechanism occurs in ADPKD to shut down ASS1 expression. Evaluation of human ADPKD and *Pkd1*$^{flox/flox}$*:Pkhd1-Cre* tissues, with human and mouse RCC as positive controls, showed no methylation of the *ASS1* promoter in ADPKD (Fig. 6). Thus, the loss of expression of this enzyme may be in part due to atrophy of high hASS1/mAss1 expressing proximal tubule cells in cystic kidneys (see above and Figs. 2 and 3).

Since all of the ADPKD cell lines and tissues studied expressed decreased levels of ASS1 protein as compared to "normal" cells and tissues, which implies arginine auxotrophy in ADPKD, we asked whether there was an effect of media arginine depletion on proliferation of these cells. When grown in several concentrations of media arginine, there was a differential effect between *Pkd1*-null and wild-type growth and viability in both cell lines, with the *Pkd1*-null cells displaying significantly less growth and viability with decreased arginine concentrations compared to the wild-type cells (Fig. 7). The PN24 cells were significantly more growth inhibited than PH2 cells when grown in 0-0.01 mM arginine (Fig. 7a) while the MEK *Pkd1*-null cells were significantly more growth inhibited than MEK WT cells when grown in 0.001-0.1 mM arginine (Fig. 7b).

The arginine EC50s were higher in the *Pkd1*-null cell lines compared to their respective wild-type cell line in both MTT and methylene blue assays (Table 1). The EC50s also confirm that the embryonic MEK *Pkd1*-null cells with lower expression of mAss1 (Fig. 1a) were more sensitive to arginine deprivation than the adult *Pkd1*-null cells (PN24).

To determine whether arginine depletion decreases cystogenesis, we first utilized an *in vitro* matrigel-based approach(12). The two *Pkd1*-null cell lines grew larger cysts than their WT control lines ($p<0.05$; Fig. 8). The PH2 cell line grew very few cysts (data not shown) and the size was mostly unaffected by arginine concentration (Fig. 8). The growth of PN24, MEK *Pkd1*-null and MEK-WT cysts was not decreased by culturing in 0.1 mM compared to 0.7 mM arginine but in all three lines cysts were significantly smaller in 0.01 mM compared to 0.1 mM and smaller again in 0.001 mM compared to 0.01 mM arginine. MEK *Pkd1*-null cysts were also significantly smaller in 0 mM compared to 0.001mM arginine (Fig. 8). Thus, arginine-dependent cystogenesis in PKD-model cells parallels changes in growth and viability, all phenomena being more pronounced in these cells than in normal cells.

Next, we tested the effects of arginine depletion in an already established(2, 26, 42) *ex vivo* cystogenesis assay using metanephric organ cultures(17). Under basal culture conditions, wild-type kidneys from embryonic day 13.5 mice grow in size and continue ureteric bud branching and tubule formation over a 4- to 5-day period. Treatment of these kidneys with cyclic AMP (cAMP) analogues induces the formation of cysts, which continue to enlarge over several days. Incubation of kidneys in medium containing the normal concentration of arginine for 5 days in the presence of exogenous cAMP resulted in significant cyst formation (Fig. 9). In contrast, reduction in media

arginine concentration (to 50% and 25% of normal, respectively) attenuated cystogenesis in an arginine dose-dependent manner (Fig. 9).

To begin to evaluate a mechanism and rationale for arginine auxotrophy in ADPKD cells, we used a non-targeted metabolomics approach similar to what we have previously accomplished in several ARPKD studies(16, 43). We grew the cells in arginine-deficient media which served to amplify the specific effect of an arginine-deficient environment, and we compared the metabolome of all four cell lines grown in arginine-deficient to those grown in arginine-replete media (Supplemental Table 3). Of the many cell-type differences occurring in primary metabolite levels after 18 hours of culture with or without arginine, the most consistent changes with arginine depletion were those in amino acid metabolism pathways, with glutamine and proline pathways being the most affected (Supplemental Table 3; Fig. 10). Strikingly, cellular glutamine was increased with arginine deprivation in all cell lines up to 25.1-fold ($p \leq 0.02$; Supplemental Table 3), while oxoproline and trans-4-hydroxyproline were increased up to 6.7-fold ($p \leq 0.02$). Only acylcarnitine (C2:0) and citric acid were decreased in all cell lines ($p \leq 0.02$). Hippuric acid, pyruvate, and beta-alanine were all decreased in 3 of the 4 cell lines ($p \leq 0.04$; Fig. 10). Intriguingly, arginine, citrulline, ornithine, alpha-ketoglutarate and lysine were decreased only in the PH2/PN24 cells, while ornithine was actually increased 2-3-fold ($p \leq 0.06$) in MEK-WT and *Pkd1*-null cells with arginine depletion (Supplemental Table 3). This may indicate that embryonic kidney cells in the collecting ducts (MEK) are more efficient at (1) conserving arginine, (2) transporting citrulline and the remaining arginine from the arginine deficient media, and/or (3) converting citrulline into arginine and ornithine.

To validate the glutamine finding, we used arginine deiminase (ADI) to attenuate arginine in normal media (Fig. 11a). *Pkd1*-null cells (with decreased ASS1) grown in this media produced more glutamate than their wild-type counterparts (Fig. 11b). Given the requirement for glutamine (which is converted to glutamate by glutaminase in kidney cells) in some models of PKD(16), and that arginine synthesis can be augmented by available glutamine(44), we propose that ASS1 deficiency increases the uptake and/or utilization of glutamine for cyst growth at the expense of arginine auxotrophy.

DISCUSSION

Arginine is classified as a semi-essential or conditionally essential amino acid, depending on the developmental stage as well as the health status of the individual. Normal kidney cells make arginine from citrulline, and arginine is converted to ornithine by arginase. Ornithine can subsequently be converted into glutamate, glutamine, alpha-ketoglutarate, gamma-aminobutyric acid, or putrescine(23). Preterm infants are unable to synthesize arginine, and adult burn patients have a higher than normal requirement for arginine(51, 52) making the amino acid nutritionally essential for these individuals. The finding that arginine is essential for many malignancies may reflect the “stem-ness” of this disease and its relationship to an earlier developmental stage(3). Given the similarity of PKD to the malignant process(40), it is fascinating that a similar arginine auxotrophic phenomenon (36, 46, 49, 50) appears to be occurring in cystogenesis.

We have studied the expression of ASS1 at the cellular level in human ADPKD and a mouse model of ADPKD. In human ADPKD it is likely that atrophy of the proximal tubules, which is concomitant with cystogenesis(31), is responsible for the loss of a

significant number of ASS1 expressing cells. In the mouse model we hypothesize that the development of cysts and concomitant fibrosis of the kidney, which is known to result in a reduction in healthy tubular tissue(14) results in a loss of ASS1 expressing proximal tubules. Cysts start to develop after P10 in the $Pkd1^{floxflox}$:Pkhd1-Cre mice and we found that mAss1 did not decrease until sometime between P14 and P21. This loss of mAss1 expression was mostly due to cystogenesis, not Pkd1 expression levels, as the $Pkd1^{+/flox}$:Pkhd1-Cre mice didn't have a significant decrease in mAss1 by P21. Consistent with this finding mAss1 expression is also lower in early cystic kidneys of the AQP11-null mouse(39). These mice develop proximal tubule cysts at around 21 days due to a perturbation of polycystin 1 trafficking and are dead by 30 days of age. It is possible that Ass1 protein levels were affected very early in the AQP11-null model because the cysts form in the proximal tubules which are the main cell type that produces Ass1.

It is likely that arginine reprogramming in PKD, concomitant with a loss of the ASS1 expressing cells in cystic tissue, results in some advantage in another metabolic pathway that allows cystic epithelia to proliferate and/or escape normal cell death pathways. Extant data suggest a variety of mechanisms by which arginine depletion may lead to "success" in cancer, such as accumulated aspartate being available for pyrimidine synthesis(37), accumulation of ornithine which can then be applied to polyamine production(33), and even modulation of T-cell activity contributing to decreased anti-tumor activity(9).

Our non-targeted metabolomics analyses did not show consistent differences in the metabolome of Pkd1-null vs WT cells. We postulate that this is due to (1)

differences in the basic metabolism of embryonic collecting duct (MEK) vs. adult (PH2/PN24) proximal tubule kidney cells or (2) the lack of a “true” WT adult kidney cell to use as a comparator for the PN24 cells, given that the PH2 cells are heterozygous for the *Pkd1* gene and (3) much lower levels of mAss1 in MEK Pkd1-null vs PN24 Pkd1-null cells. However, and most strikingly, we did find significant effects of arginine depletion on various metabolites, five of which were consistently changed in all four cell lines studied and thus they are generalizable to renal tubular cell biology in the presence of arginine deficiency (which is a model for arginine auxotrophy which would be present in PKD cells in the absence of ASS1). Glutamine is one of the cellular metabolites that was increased with arginine deficiency. Since the kidney is very efficient at transporting amino acids(4), it is tempting to speculate that arginine deprivation results in an increased uptake of glutamine to act as a substrate to make citrulline and thus arginine(44). In light of our previous glutamine data in ARPKD(16) and abundant data from us and others in RCC(1, 47, 48), it is likely that decreasing synthesis of arginine through decreased ASS1 expression leads to a reliance on glutamine, which is consistent with possible glutamine addiction in PKD. Such a possibility is currently being evaluated using the glutaminase inhibitor CB839(10, 28) in our laboratories.

We further hypothesize that media arginine depletion leads alterations in proline metabolism. For example, ornithine could be converted in the mitochondria to 1-pyrroline-5-carboxylate which can be transported to the cytosol and converted to proline(20), which can be further catabolized to 4-hydroxyproline, which we observed to be increased with arginine depletion. The increase in 5-oxoproline, which can be

synthesized from glutathione, also potentially contributes to the observed buildup of 4-hydroxyproline. Interestingly, proline hydroxylation is a hallmark of hypoxic response in many cancers(18, 19) and has been shown to regulate Akt(11) and in a very recent study, arginine deficiency was reported to promote Akt phosphorylation at Serine 473 by mTORC2(29), perhaps by involving the prolyl hydroxylase pathway. Thus, our metabolomics data demonstrates a link between arginine depletion, ASS1 deficiency, and proline hydroxylation in the PKD hypoxic response.

The fact that arginine, in adult tissues, is likely essential only in a limited number of tissues including cystic epithelia (as well as any possible existing malignancies), makes arginine reductive therapies promising and likely to have minimal if any adverse effects. Dietary arginine is not required by healthy subjects and is conditionally indispensable only for severely stressed patients(52). While protein restricted diets have been inhibitory for tumor growth in some mouse models of cancer(53), dietary depletion of arginine, certainly for the length of time that would be required in a PKD patient, is likely not feasible since this amino acid is of course found in many proteins. However, enzymatic methods to specifically target arginine have been used in multiple clinical trials. Three arginine-degrading enzymes have been investigated for treating cancers auxotrophic for arginine. These are mycoplasma arginine deiminase (ADI), recombinant human arginase (rhArgI) and arginine decarboxylase(32). Of these three, arginine decarboxylase produces toxic by-products, while ADI is more effective than rhArgI at overcoming the physiological mechanisms of arginine homeostasis and reducing serum arginine concentrations(32). While arginine-deiminase coupled to PEG (ADI-PEG) did not meet its primary endpoint of demonstrating overall survival benefits in advanced

hepatocellular carcinoma, this drug was well tolerated, with the most common side effects being fatigue and decrease of appetite (www.polarispharma.com). Our demonstration of lack of toxicity of arginine depletion in ex vivo cystogenesis assays supports the likely safety of arginine deiminase treatment in PKD.

In summary we have demonstrated that both mouse models and human ADPKD tissue have reduced ASS1 expression, and arginine depletion results in decreased cyst formation. Given the fact that arginine is an essential amino acid only in tissues in which ASS1 is attenuated, such as PKD kidneys and some tumors, this newly discovered occurrence of arginine auxotrophy in PKD suggests a novel therapeutic approach using dietary means or arginine deiminase therapies.

ACKNOWLEDGEMENTS

We thank Shreeya Joshee and Avneet Shaheed for invaluable assistance with some of the experiments in this study.

GRANTS

This work was supported by NIH grants 1R03CA181837-01 and 1R01DK082690-01A1, the Medical Service of the US Department of Veterans' Affairs, and Dialysis Clinics, Inc. (DCI) (all to R.H. Weiss); and NIH grant 1R01DK108005-02 (to M.R. Mahjoub). Targeted metabolite analysis was performed under the auspices of the U.S.

Department of Energy by Lawrence Livermore National Laboratory (LLNL) under Contract DE-AC52-07NA27344 with support from NIGMS grant P41GM103483.

DISCLOSURES

This work was in part support by grants from Dialysis Clinics Incorporated (DCI), but DCI had no influence on the experiments, data collection, or manuscript writing.

REFERENCES

1. Abu Aboud O, Habib SL, Trott JF, Stewart B, Liang S, Chaudhari AJ, Sutcliffe JL, and Weiss RH. Glutamine addiction in kidney cancer suppresses oxidative stress and can be exploited for real-time imaging. *Cancer Res* 77: 6746-6758, 2017.
2. Anders C, Ashton N, Ranjzad P, Dilworth MR, and Woolf AS. Ex vivo modeling of chemical synergy in prenatal kidney cystogenesis. *PLoS One* 8: e57797, 2013.
3. Barak H, Huh SH, Chen S, Jeanpierre C, Martinovic J, Parisot M, Bole-Feysot C, Nitschke P, Salomon R, Antignac C, Ornitz DM, and Kopan R. FGF9 and FGF20 maintain the stemness of nephron progenitors in mice and man. *Dev Cell* 22: 1191-1207, 2012.
4. Brosnan ME, and Brosnan JT. Renal arginine metabolism. *J Nutr* 134: 2791S-2795S, 2004.
5. Byrne K, Cheng X, Vierck J, Erickson S, Green E, Duckett S, and Dodson M. Use of a 96-well plate reader to evaluate proliferation of equine satellite cell clones in vitro. *Methods Cell Sci* 19: 311-316, 1998.
6. de Jonge HJ, Fehrmann RS, de Bont ES, Hofstra RM, Gerbens F, Kamps WA, de Vries EG, van der Zee AG, te Meerman GJ, and ter Elst A. Evidence based selection of housekeeping genes. *PLoS One* 2: e898, 2007.
7. Everaert BR, Boulet GA, Timmermans JP, and Vrints CJ. Importance of suitable reference gene selection for quantitative real-time PCR: special reference to mouse myocardial infarction studies. *PLoS One* 6: e23793, 2011.
8. Ganti S, Taylor SL, Abu AO, Yang J, Evans C, Osier MV, Alexander DC, Kim K, and Weiss RH. Kidney tumor biomarkers revealed by simultaneous multiple matrix metabolomics analysis. *Cancer Res* 72: 3471-3479, 2012.
9. Geiger R, Rieckmann JC, Wolf T, Basso C, Feng Y, Fuhrer T, Kogadeeva M, Picotti P, Meissner F, Mann M, Zamboni N, Sallusto F, and Lanzavecchia A. L-Arginine Modulates T Cell Metabolism and Enhances Survival and Anti-tumor Activity. *Cell* 167: 829-842, 2016.
10. Gross MI, Demo SD, Dennison JB, Chen L, Chernov-Rogan T, Goyal B, Janes JR, Laidig GJ, Lewis ER, Li J, Mackinnon AL, Parlati F, Rodriguez ML, Shwonek PJ, Sjogren EB, Stanton TF, Wang T, Yang J, Zhao F, and Bennett MK. Antitumor activity of the glutaminase inhibitor CB-839 in triple-negative breast cancer. *Mol Cancer Ther* 13: 890-901, 2014.
11. Guo J, Chakraborty AA, Liu P, Gan W, Zheng X, Inuzuka H, Wang B, Zhang J, Zhang L, Yuan M, Novak J, Cheng JQ, Toker A, Signoretti S, Zhang Q, Asara JM, Kaelin WG, Jr., and Wei W. pVHL suppresses kinase activity of Akt in a proline-hydroxylation-dependent manner. *Science* 353: 929-932, 2016.
12. Guo Q, Xia B, Moshiach S, Xu C, Jiang Y, Chen Y, Sun Y, Lahti JM, and Zhang XA. The microenvironmental determinants for kidney epithelial cyst morphogenesis. *Eur J Cell Biol* 87: 251-266, 2008.
13. Guo S, Duan JA, Qian D, Tang Y, Qian Y, Wu D, Su S, and Shang E. Rapid determination of amino acids in fruits of Ziziphus jujuba by hydrophilic interaction ultra-high-performance liquid chromatography coupled with triple-quadrupole mass spectrometry. *J Agric Food Chem* 61: 2709-2719, 2013.
14. Happe H, van der Wal AM, Salvatori DC, Leonhard WN, Breuning MH, de Heer E, and Peters DJ. Cyst expansion and regression in a mouse model of polycystic kidney disease. *Kidney Int* 83: 1099-1108, 2013.
15. Huang HY, Wu WR, Wang YH, Wang JW, Fang FM, Tsai JW, Li SH, Hung HC, Yu SC, Lan J, Shiue YL, Hsing CH, Chen LT, and Li CF. ASS1 as a novel tumor suppressor gene in myxofibrosarcomas: aberrant loss via epigenetic DNA methylation confers aggressive

phenotypes, negative prognostic impact, and therapeutic relevance. *Clin Cancer Res* 19: 2861-2872, 2013.
16. Hwang VJ, Kim J, Rand A, Yang C, Sturdivant S, Hammock B, Bell PD, Guay-Woodford LM, and Weiss RH. The cpk model of recessive PKD shows glutamine dependence associated with the production of the oncometabolite 2-hydroxyglutarate. *Am J Physiol Renal Physiol* 309: F492-F498, 2015.
17. Hwang VJ, Zhou X, Chen X, Trott J, Abu Aboud O, Shim K, Dionne LK, Chmiel KJ, Senapedis W, Baloglu E, Mahjoub MR, Li X, and Weiss RH. Anticystogenic activity of a small molecule PAK4 inhibitor may be a novel treatment for autosomal dominant polycystic kidney disease. *Kidney Int* 92: 922-933, 2017.
18. Ivan M, Kondo K, Yang H, Kim W, Valiando J, Ohh M, Salic A, Asara JM, Lane WS, and Kaelin WG, Jr. HIFalpha targeted for VHL-mediated destruction by proline hydroxylation: implications for O2 sensing. *Science* 292: 464-468, 2001.
19. Jaakkola P, Mole DR, Tian YM, Wilson MI, Gielbert J, Gaskell SJ, von Kriegsheim A, Hebestreit HF, Mukherji M, Schofield CJ, Maxwell PH, Pugh CW, and Ratcliffe PJ. Targeting of HIF-alpha to the von Hippel-Lindau ubiquitylation complex by O2-regulated prolyl hydroxylation. *Science* 292: 468-472, 2001.
20. Jones ME. Conversion of glutamate to ornithine and proline: pyrroline-5-carboxylate, a possible modulator of arginine requirements. *J Nutr* 115: 509-515, 1985.
21. Kouadjo KE, Nishida Y, Cadrin-Girard JF, Yoshioka M, and St-Amand J. Housekeeping and tissue-specific genes in mouse tissues. *BMC genomics* 8: 127, 2007.
22. Lan J, Tai HC, Lee SW, Chen TJ, Huang HY, and Li CF. Deficiency in expression and epigenetic DNA Methylation of ASS1 gene in nasopharyngeal carcinoma: negative prognostic impact and therapeutic relevance. *Tumour Biol* 35: 161-169, 2014.
23. Levillain O, Hus-Citharel A, Garvi S, Peyrol S, Reymond I, Mutin M, and Morel F. Ornithine metabolism in male and female rat kidney: mitochondrial expression of ornithine aminotransferase and arginase II. *Am J Physiol Renal Physiol* 286: F727-738, 2004.
24. Li LC, and Dahiya R. MethPrimer: designing primers for methylation PCRs. *Bioinformatics* 18: 1427-1431, 2002.
25. Long Y, Tsai WB, Wangpaichitr M, Tsukamoto T, Savaraj N, Feun LG, and Kuo MT. Arginine deiminase resistance in melanoma cells is associated with metabolic reprogramming, glucose dependence, and glutamine addiction. *Mol Cancer Ther* 12: 2581-2590, 2013.
26. Magenheimer BS, St John PL, Isom KS, Abrahamson DR, De Lisle RC, Wallace DP, Maser RL, Grantham JJ, and Calvet JP. Early embryonic renal tubules of wild-type and polycystic kidney disease kidneys respond to cAMP stimulation with cystic fibrosis transmembrane conductance regulator/Na(+),K(+),2Cl(-) Co-transporter-dependent cystic dilation. *J Am Soc Nephrol* 17: 3424-3437, 2006.
27. McAlpine JA, Lu HT, Wu KC, Knowles SK, and Thomson JA. Down-regulation of argininosuccinate synthetase is associated with cisplatin resistance in hepatocellular carcinoma cell lines: implications for PEGylated arginine deiminase combination therapy. *BMC Cancer* 14: 621, 2014.
28. Meric-Bernstam F, Tannir NM, Mier JW, DeMichele A, Telli ML, Fan AC, Munster PN, Carvajal RD, Orford KW, Bennett MK, Iliopoulos O, Owonikoko TK, Patel MR, McKay R, Infante JR, Voss MH, and Harding JJ. Phase 1 study of CB-839, a small molecule inhibitor of glutaminase (GLS), alone and in combination with everolimus (E) in patients (pts) with renal cell cancer (RCC). *J Clin Oncol* 34: 4568-4568, 2016.
29. Miyamoto T, Lo PHY, Saichi N, Ueda K, Hirata M, Tanikawa C, and Matsuda K. Argininosuccinate synthase 1 is an intrinsic Akt repressor transactivated by p53. *Sci Adv* 3: e1603204, 2017.

30. Nauli SM, Alenghat FJ, Luo Y, Williams E, Vassilev P, Li X, Elia AE, Lu W, Brown EM, Quinn SJ, Ingber DE, and Zhou J. Polycystins 1 and 2 mediate mechanosensation in the primary cilium of kidney cells. *Nat Genet* 33: 129-137, 2003.
31. Norman J. Fibrosis and progression of autosomal dominant polycystic kidney disease (ADPKD). *Biochimica et biophysica acta* 1812: 1327-1336, 2011.
32. Patil MD, Bhaumik J, Babykutty S, Banerjee UC, and Fukumura D. Arginine dependence of tumor cells: targeting a chink in cancer's armor. *Oncogene* 35: 4957-4972, 2016.
33. Pavlova NN, and Thompson CB. The Emerging Hallmarks of Cancer Metabolism. *Cell Metab* 23: 27-47, 2016.
34. Perroud B, Ishimaru T, Borowsky AD, and Weiss RH. Grade-dependent proteomics characterization of kidney cancer. *Mol Cell Proteomics* 8: 971-985, 2008.
35. Piontek K, Menezes LF, Garcia-Gonzalez MA, Huso DL, and Germino GG. A critical developmental switch defines the kinetics of kidney cyst formation after loss of Pkd1. *Nat Med* 13: 1490-1495, 2007.
36. Qiu F, Chen YR, Liu X, Chu CY, Shen LJ, Xu J, Gaur S, Forman HJ, Zhang H, Zheng S, Yen Y, Huang J, Kung HJ, and Ann DK. Arginine starvation impairs mitochondrial respiratory function in ASS1-deficient breast cancer cells. *Sci Signal* 7: ra31, 2014.
37. Rabinovich S, Adler L, Yizhak K, Sarver A, Silberman A, Agron S, Stettner N, Sun Q, Brandis A, Helbling D, Korman S, Itzkovitz S, Dimmock D, Ulitsky I, Nagamani SC, Ruppin E, and Erez A. Diversion of aspartate in ASS1-deficient tumours fosters de novo pyrimidine synthesis. *Nature* 527: 379-383, 2015.
38. Rowe I, Chiaravalli M, Mannella V, Ulisse V, Quilici G, Pema M, Song XW, Xu H, Mari S, Qian F, Pei Y, Musco G, and Boletta A. Defective glucose metabolism in polycystic kidney disease identifies a new therapeutic strategy. *Nat Med* 19: 488-493, 2013.
39. Saito T, Tanaka Y, Morishita Y, and Ishibashi K. Proteomic analysis of AQP11-null kidney: Proximal tubular type polycystic kidney disease. *Biochemistry and Biophysics Reports* 13: 17-21, 2018.
40. Seeger-Nukpezah T, Geynisman DM, Nikonova AS, Benzing T, and Golemis EA. The hallmarks of cancer: relevance to the pathogenesis of polycystic kidney disease. *Nat Rev Nephrol* 11: 515-534, 2015.
41. Shibazaki S, Yu Z, Nishio S, Tian X, Thomson RB, Mitobe M, Louvi A, Velazquez H, Ishibe S, Cantley LG, Igarashi P, and Somlo S. Cyst formation and activation of the extracellular regulated kinase pathway after kidney specific inactivation of Pkd1. *Hum Mol Genet* 17: 1505-1516, 2008.
42. Su L, Liu L, Jia Y, Lei L, Liu J, Zhu S, Zhou H, Chen R, Lu HAJ, and Yang B. Ganoderma triterpenes retard renal cyst development by downregulating Ras/MAPK signaling and promoting cell differentiation. *Kidney Int* 92: 1404-1418, 2017.
43. Taylor SL, Ganti S, Bukanov NO, Chapman A, Fiehn O, Osier M, Kim K, and Weiss RH. A metabolomics approach using juvenile cystic mice to identify urinary biomarkers and altered pathways in polycystic kidney disease. *Am J Physiol Renal Physiol* 298: F909-F922, 2010.
44. Tomlinson C, Rafii M, Ball RO, and Pencharz P. Arginine synthesis from enteral glutamine in healthy adults in the fed state. *Am J Physiol Endocrinol Metabol* 301: E267-273, 2011.
45. Trott JF, Kim J, Aboud OA, Wettersten H, Stewart B, Berryhill G, Uzal F, Hovey RC, Chen CH, Anderson K, Graef A, Sarver AL, Modiano JF, and Weiss RH. Inhibiting tryptophan metabolism enhances interferon therapy in kidney cancer. *Oncotarget* 7: 66540-66557, 2016.
46. Wettersten HI, Aboud OA, Lara PN, Jr., and Weiss RH. Metabolic reprogramming in clear cell renal cell carcinoma. *Nat Rev Nephrol* 13: 410-419, 2017.
47. Wise DR, DeBerardinis RJ, Mancuso A, Sayed N, Zhang XY, Pfeiffer HK, Nissim I, Daikhin E, Yudkoff M, McMahon SB, and Thompson CB. Myc regulates a transcriptional

program that stimulates mitochondrial glutaminolysis and leads to glutamine addiction. *Proc Natl Acad Sci U S A* 105: 18782-18787, 2008.
48. Wise DR, and Thompson CB. Glutamine addiction: a new therapeutic target in cancer. *Trends Biochem Sci* 35: 427-433, 2010.
49. Yoon CY, Shim YJ, Kim EH, Lee JH, Won NH, Kim JH, Park IS, Yoon DK, and Min BH. Renal cell carcinoma does not express argininosuccinate synthetase and is highly sensitive to arginine deprivation via arginine deiminase. *Int J Cancer* 120: 897-905, 2007.
50. Yoon JK, Frankel AE, Feun LG, Ekmekcioglu S, and Kim KB. Arginine deprivation therapy for malignant melanoma. *Clin Pharmacol* 5: 11-19, 2013.
51. Yu YM, Ryan CM, Burke JF, Tompkins RG, and Young VR. Relations among arginine, citrulline, ornithine, and leucine kinetics in adult burn patients. *Am J Clin Nutr* 62: 960-968, 1995.
52. Yu YM, Ryan CM, Castillo L, Lu XM, Beaumier L, Tompkins RG, and Young VR. Arginine and ornithine kinetics in severely burned patients: increased rate of arginine disposal. *Am J Physiol Endocrinol Metabol* 280: E509-517, 2001.
53. Zam W. Arginine enzymatic deprivation and diet restriction for cancer treatment. *Braz J Pharm Sci* 53: e00200, 2017.
54. Zhou X, Fan LX, Sweeney WE, Jr., Denu JM, Avner ED, and Li X. Sirtuin 1 inhibition delays cyst formation in autosomal-dominant polycystic kidney disease. *J Clin Invest* 123: 3084-3098, 2013.

640 **Table 1.** EC50 for arginine dose (mM) calculated for the *Pkd1*-null and WT cell lines
641 measured using the MTT and methylene blue assays.
642

	MTT	Methylene Blue
MEK-wt	0.0084 mM	0.0068 mM
MEK-null	0.22 mM	0.15 mM
PH2	0.0024 mM	0.0052 mM
PN24	0.0081 mM	0.009 mM

643

644 FIGURE LEGENDS

645

646 1. ASS1 protein is decreased in polycystic kidney disease (PKD).

647 Protein was prepared and immunoblotted for ASS1 and/or β-actin or vinculin.

648 ImageJ or FujiFilm LAS-4000 quantification of protein expression, corrected for the

649 reference protein(s), are next to the blots. RNA was extracted, reverse transcribed

650 and subjected to qPCR for m*Ass1* mRNA (corrected for *Eef2, Rpl13a and Rn18S*

651 mRNA levels) or *hASS1* mRNA (corrected for *PPIA*, *RPS13* and *RNA18S5*).

652 Statistically significant differences in ASS1 protein and mRNA expression are

653 indicated on the graphs. Immunoblots are representative of at least two repeats.

654 a) Mouse embryonic kidney (MEK) wild-type (WT), *Pkd1*-null (MEK null) cell lines

655 and postnatal mouse *Pkd1*-heterozygous (PH2) and *Pkd1*-null (PN24) kidney cell

656 lines were harvested for protein and RNA at confluence in triplicate wells. Data are

657 means ± SD.

658 b) Protein and RNA was extracted from adult Balb/cJ (n=3), day 25 $Pkd1^{+/+}$*:Pkhd1-*

659 *Cre* ($Pkd1^{+/+}$; n=3) and day 25 $Pkd1^{flox/flox}$*:Pkhd1*-Cre ($Pkd1^{flox/flox}$; n=3) mouse

660 kidneys. Data are means ± SD.

661 c) Protein and RNA was extracted from normal human kidneys (NHK; n=3) and

662 nephrectomy tissue from autosomal dominant PKD (ADPKD) patients (n=6) kidneys.

663 Data are means ± SD

664

665 2. ASS1 protein expression is diminished or lost in proximal tubules showing atrophy in

666 autosomal dominant polycystic kidney disease (ADPKD).

Immunohistochemical staining for human ASS1 was performed on normal human kidneys (A, C, D) and nephrectomy tissue from autosomal dominant PKD (ADPKD) patients (E, G-J) kidneys. Secondary alone controls were performed on serial sections of normal kidney tissue (B) or ADPKD tissue (F). Note that the non-atrophic tubules in ADPKD patient kidneys retain strong ASS1 protein expression.

3. Proximal tubules expressing mAss1 protein are less abundant by P14 in a mouse model of polycystic kidney disease.

Immunohistochemical staining for mouse Ass1 was performed on post-natal day 5 (P5), P10, P14 and P21 *Pkd1*$^{+/+}$*:Pkhd1-Cre* (*Pkd1*$^{+/+}$; n=3), *Pkd1*$^{+/flox}$*:Pkhd1-Cre* (*Pkd1*$^{+/flox}$; n=3) and *Pkd1*$^{flox/flox}$*:Pkhd1*-Cre (*Pkd1*$^{flox/flox}$; n=3) mouse kidneys. The secondary alone control (Neg) was on P21 *Pkd1*$^{+/+}$*:Pkhd1-Cre* kidney tissue. Note the formation of cysts by P14 as well as concomitant increase in atrophic tubules, the latter of which show diminished or loss of mAss1 protein expression.

4. mAss1 expression is significantly decreased by day 21 in the *Pkd1*$^{flox/flox}$*:Pkhd1*-Cre mouse model of polycystic kidney disease (PKD).

Protein was extracted from post-natal day 10 (P10), P14 and P21 *Pkd1*$^{+/+}$*:Pkhd1-Cre* (*Pkd1*$^{+/+}$; n=3), *Pkd1*$^{+/flox}$*:Pkhd1-Cre* (*Pkd1*$^{+/flox}$; n=3) and *Pkd1*$^{flox/flox}$*:Pkhd1*-Cre (*Pkd1*$^{flox/flox}$; n=3) mouse kidneys and immunoblotted for mASS1 and/or β-actin or vinculin. Quantification of ASS1 using the FujiFilm LAS-4000, corrected for the housekeeping protein, is next each blot.

5. mAss1 mRNA and protein expression is increased by arginine depletion in Pkd1-null cells

Protein was prepared and immunoblotted for mASS1 and β-actin and quantified as per Figure 1. RNA was extracted, reverse transcribed and subjected to qPCR for m*Ass1* mRNA and corrected for expression of three housekeeping genes as per Figure 1. Statistically significant differences in mASS1 protein and mRNA expression are indicated on the graphs.

a) PN24 and MEK *Pkd1-null* cells were cultured in low serum MEK media containing either 0.7 mM, 0.1 mM and 0 mM (PN24) or 0.001 mM (MEK *Pkd1-null*) arginine for 14 days with media changes every 2 days, then protein and RNA were extracted. Data are means ± SD (n=3).

b) PH2 and MEK-WT cells were cultured as for a). Data are means ± SD (n=3).

6. Methylation specific PCR of *hASS1* and *mAss1* reveals lack of methylation in polycystic kidney disease (PKD).

Primer sets used for amplification amplify either unmethylated (U) or methylated (M) gDNA. Bisulfite-treated gDNA from normal human kidneys, autosomal dominant PKD kidneys (ADPKD) or the renal cell carcinoma (RCC) cell line 786-O was amplified using primers specific for either U or M sequences located 300- 500 bp downstream of the *hASS1* transcription start site (TSS). Bisulfite-treated kidney gDNA from one *Pkd1*$^{+/+}$*:Pkhd1-Cre* mouse, three *Pkd1*$^{flox/flox}$*:Pkhd1-Cre* mice and the RCC cell line RENCA was amplified using primers specific for either U or M sequences located 315-213 bp upstream of the *mASS1* TSS. Neg = water control.

7. Cell proliferation is dose-dependently reduced with arginine deprivation.

a) PH2 and PN24 kidney cell lines were plated in 96-well plates ($1.5x10^3$/well), grown with various doses of arginine in the media for 5 days then assayed using MTT (viability) or methylene blue (cell number). Data are means ± SEM (n=3 experiments). *p≤0.05 compared with PH2

b) MEK WT and *Pkd1*-null kidney cell lines were plated in 96-well plates ($3x10^3$/well), grown with various doses of arginine in the media for 3 days then assayed using MTT (viability) or methylene blue (cell number). Data are means ± SEM (n=5 experiments). *p<0.05 compared with MEK WT

8. Cyst growth is inhibited with arginine deprivation.

Mouse embryonic *Pkd1*-null (MEK null), MEK WT and postnatal *Pkd1*-null (PN24) and *Pkd1*-heterozygous (PH2) kidney cells were cultured without mouse IFNγ for at least 7 days, then plated in matrigel and cultured in low serum MEK media with various concentrations of arginine. On day 13 (PN24/PH2) or 14 (MEK null/WT), cysts in matrigel were photographed (black arrows point to cysts) and diameters measured using AxioVision software (Zeiss). Data are means ± SD (n≥20) and representative of duplicate experiments.

9. Arginine depletion attenuates cAMP induced cystogenesis in ex vivo metanephric organ cultures.

Embryonic kidneys were harvested from CD1 mice at E13.5 and cultured ex vivo on Transwell membranes for 4 days. Samples were incubated in medium containing 100% (0.25 mg/ml), 50% (0.12 mg/ml) or 25% (0.06 mg/ml) arginine. Kidneys were treated with 100 μM 8-Br-cAMP to induce cystogenesis.

a) Images of kidneys taken on days 1 and 5, showing cystic progression.

b) Whole-mount immunostaining of kidneys with E-cadherin showing normal kidney development upon arginine depletion.

c) Quantification of cyst number and total cyst area in control and treated kidneys at day 5. N=4 kidneys per sample.

10. Arginine deprivation of mouse kidney cell lines affects metabolites in the urea and tricarboxylic acid cycles.

Metabolites concordantly changed in PH2, PN24, MEK WT and MEK *Pkd1*-null cells grown in 0 mM arginine media for 18 hours ($p<0.05$ in at least three cell lines) are highlighted. Red = metabolite increased with arginine deprivation. Blue = metabolite decreased with arginine deprivation.

11. Arginine deiminase substantially decreases media arginine and results in higher glutamate levels in conditioned media of *Pkd1*-null as compared to *Pkd1*-wt cells

a) Media was incubated with different concentrations of arginine deaminase (ADI) for 0-72 h and then analyzed by HPLC. Arginine concentration found to be reduced from 0.8-1 mM down to ≤0.003 mM in both medias within 24 h of ADI treatment.

b) Mouse embryonic kidney (MEK) wild-type (WT), and MEK *Pkd1*-null cells were plated and cultured in MEK media +/- ADI (2.5 µg/ml) for 24-72 h. Postnatal mouse kidney *Pkd1*-heterozygous (PH2) and *Pkd1*-null (PN24) cells were plated and cultured in PHPN media +/- ADI (2.5 µg/ml) for 72 h. Media was collected and analyzed by HPLC for glutamate. Data are means ± SD (n=3).

SUPPLEMENTAL DATA

Supplemental Table 1: PCR primers used for quantitative PCR.

Supplemental Table 2: PCR primers used for methylation specific PCR

Supplemental Table 3: Non-targeted metabolomics analysis of all four cell lines used in this study. MEK WT and *Pkd-1 null* cells (1×10^6) were grown for 18 h in MEK media with or without arginine (n=3), while PH2 and PN24 cells (1×10^6) were grown for 18 h in PHPN media with or without arginine (n=3). Cells were harvested using trypsin and snap frozen.

Sheet 1 shows significant changes in cellular metabolites of all cell lines grown in arginine complete vs arginine-depleted media. p-values and

Sheet 2 shows significant differences in metabolites for PKD-model vs PKD-wt cells in complete (arginine-replete) media that are consistent in both embryonic and adult cell lines.

Fig. 1

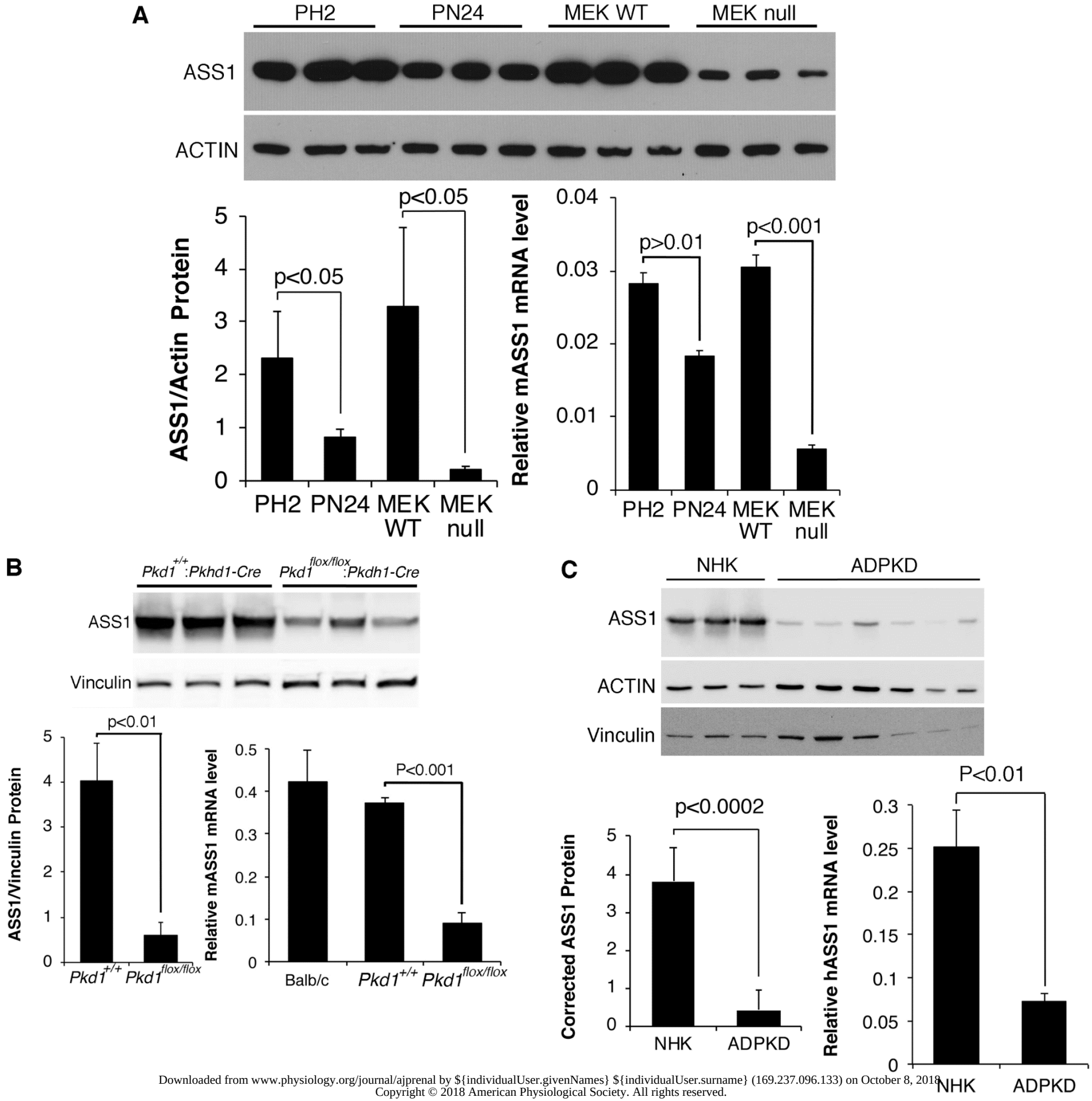

Fig. 2

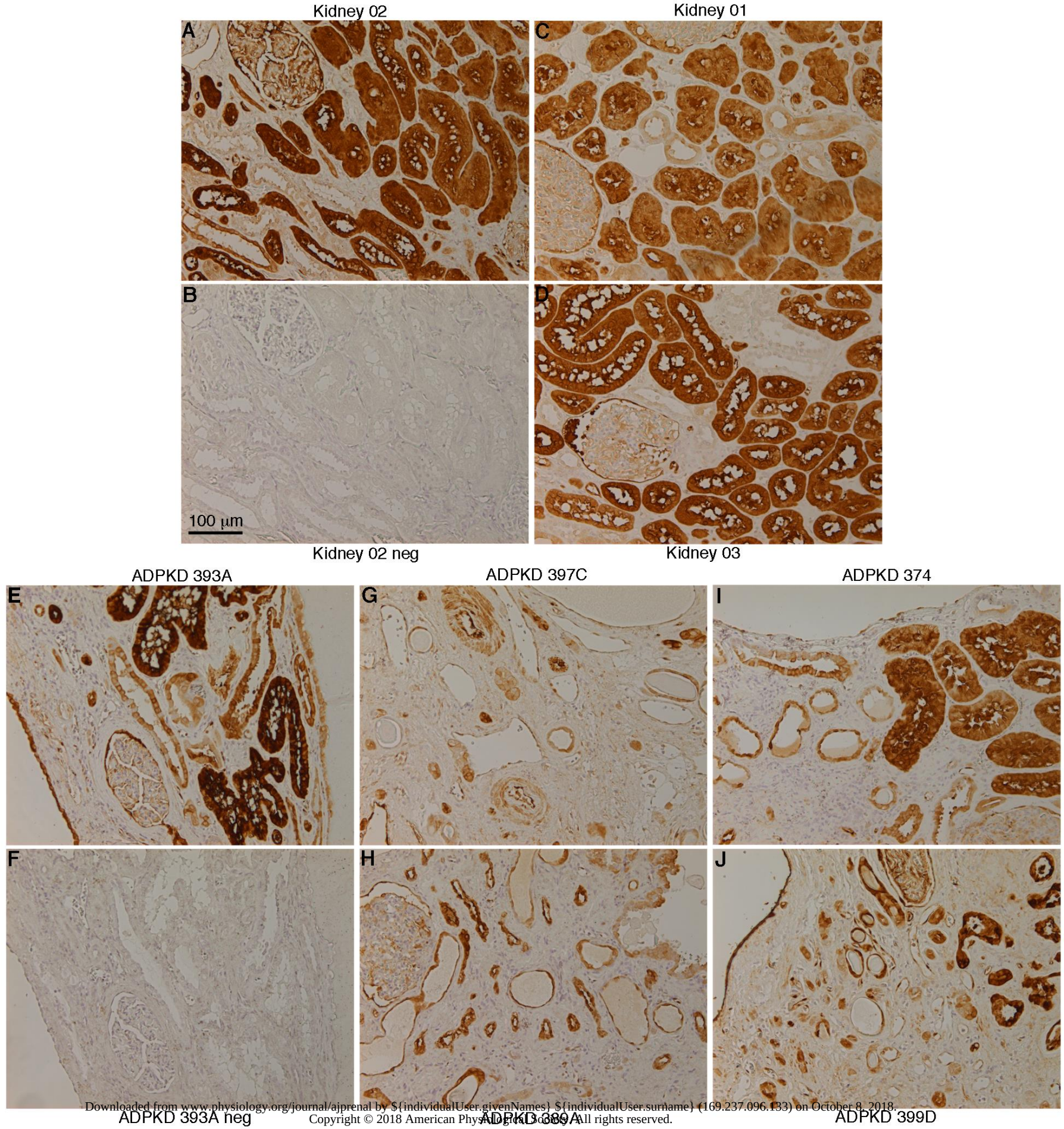

Fig. 3

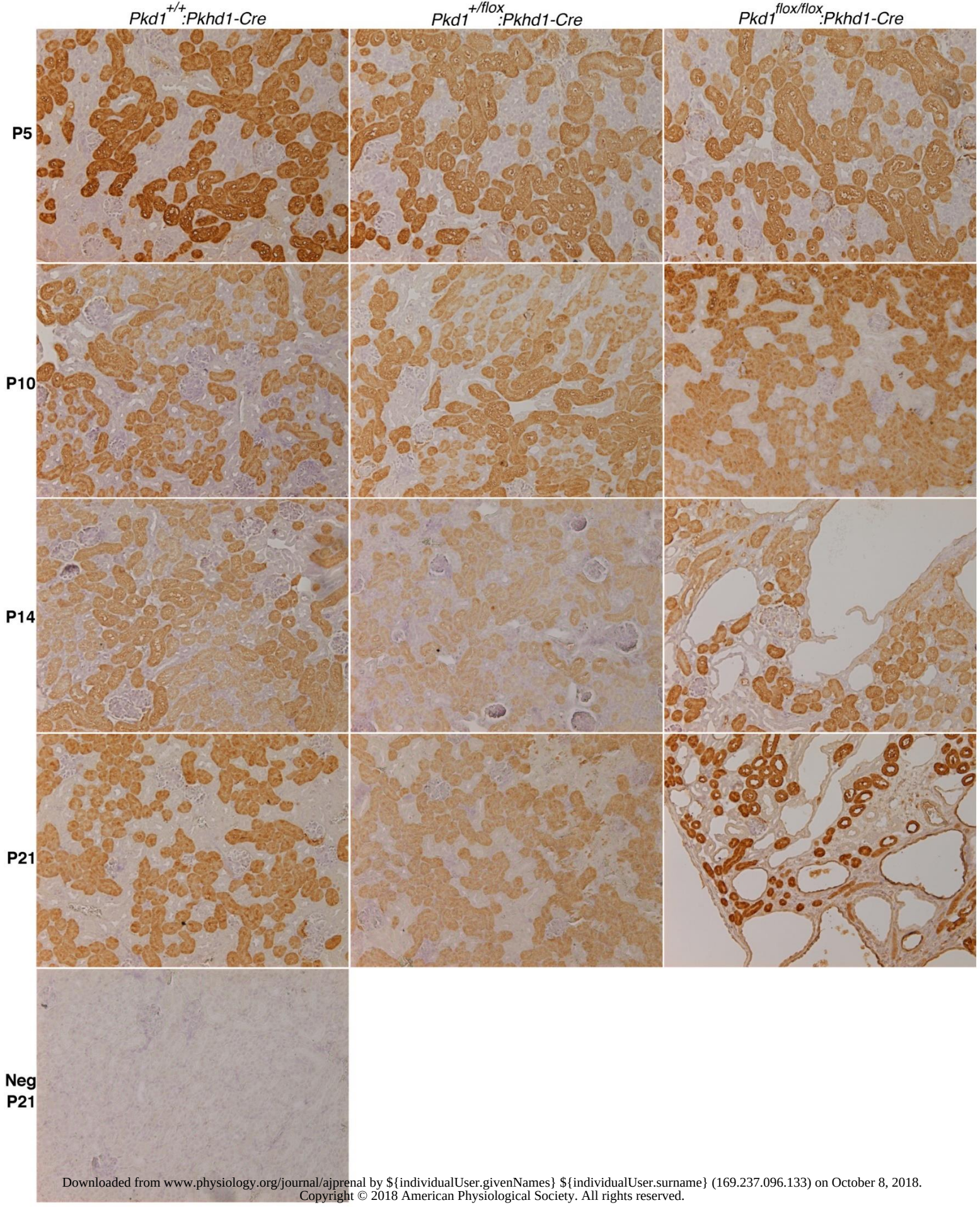

Fig. 4

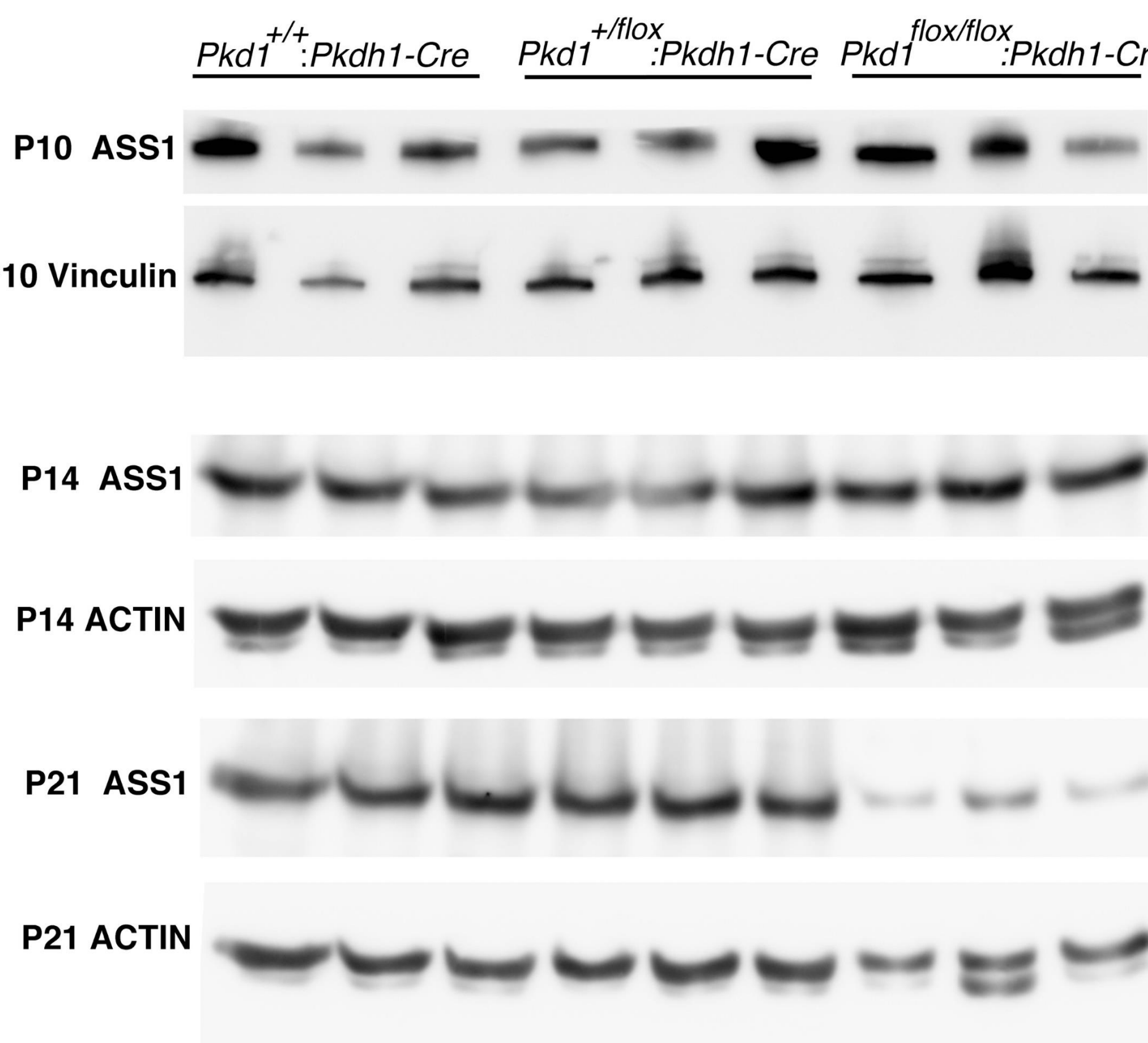

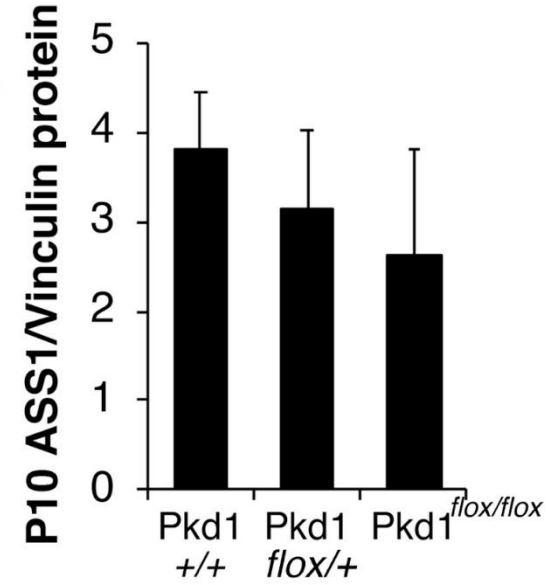

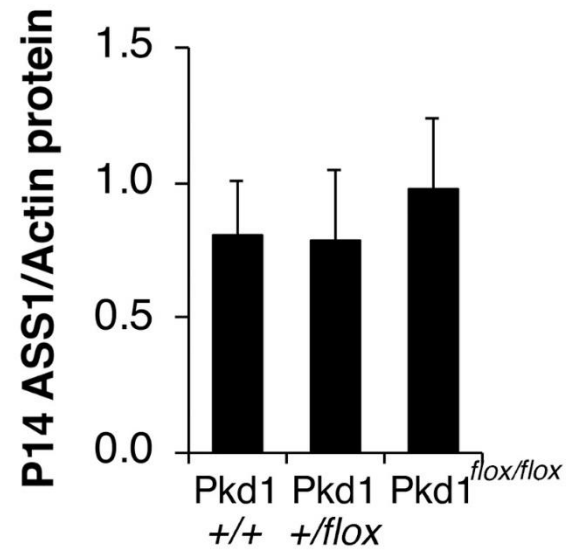

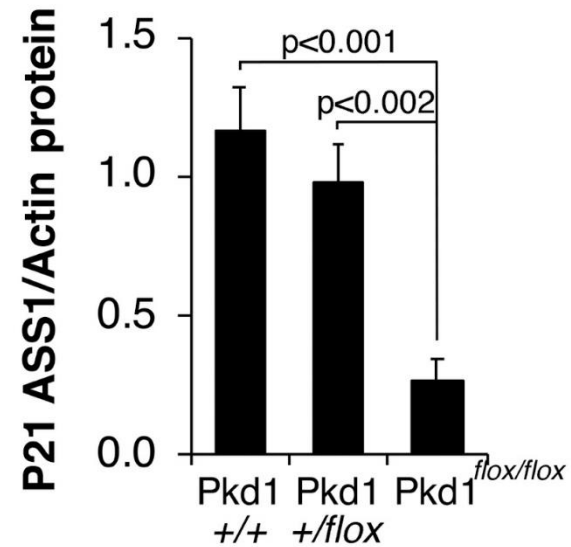

Fig. 5

a)

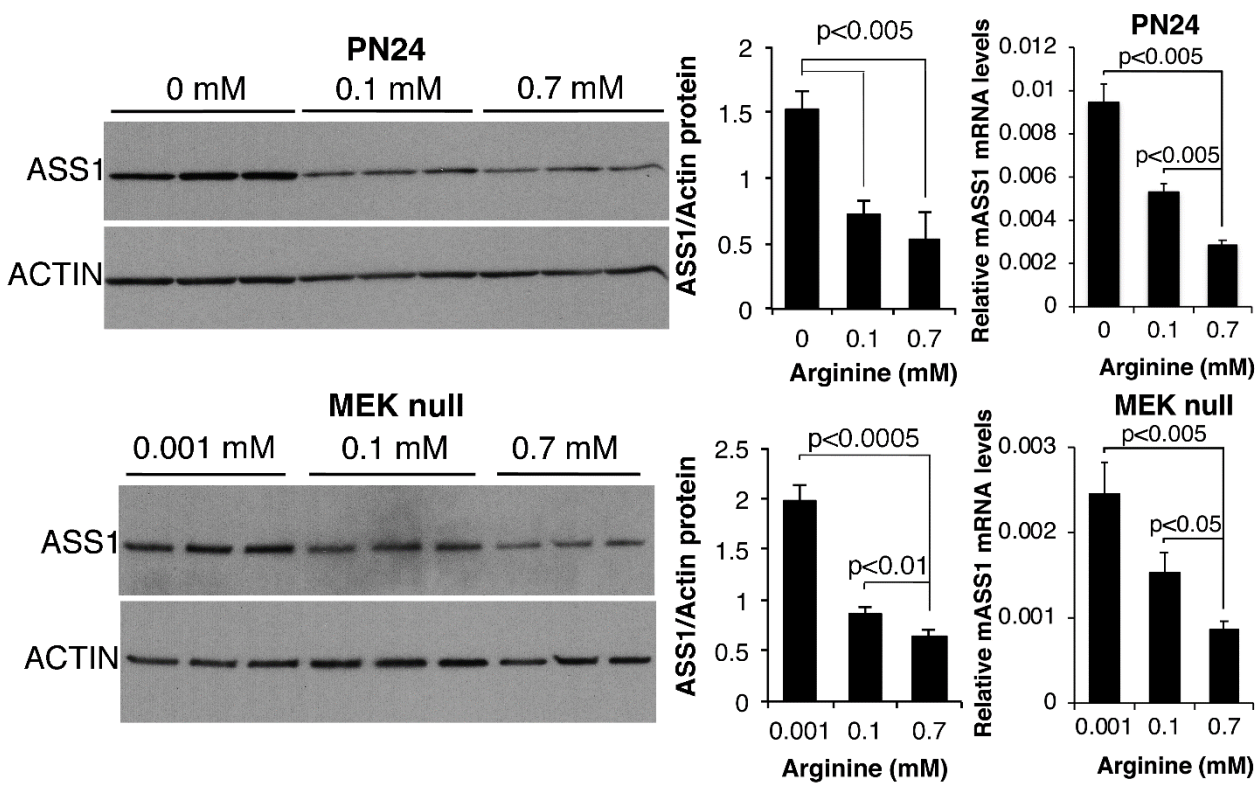

b)

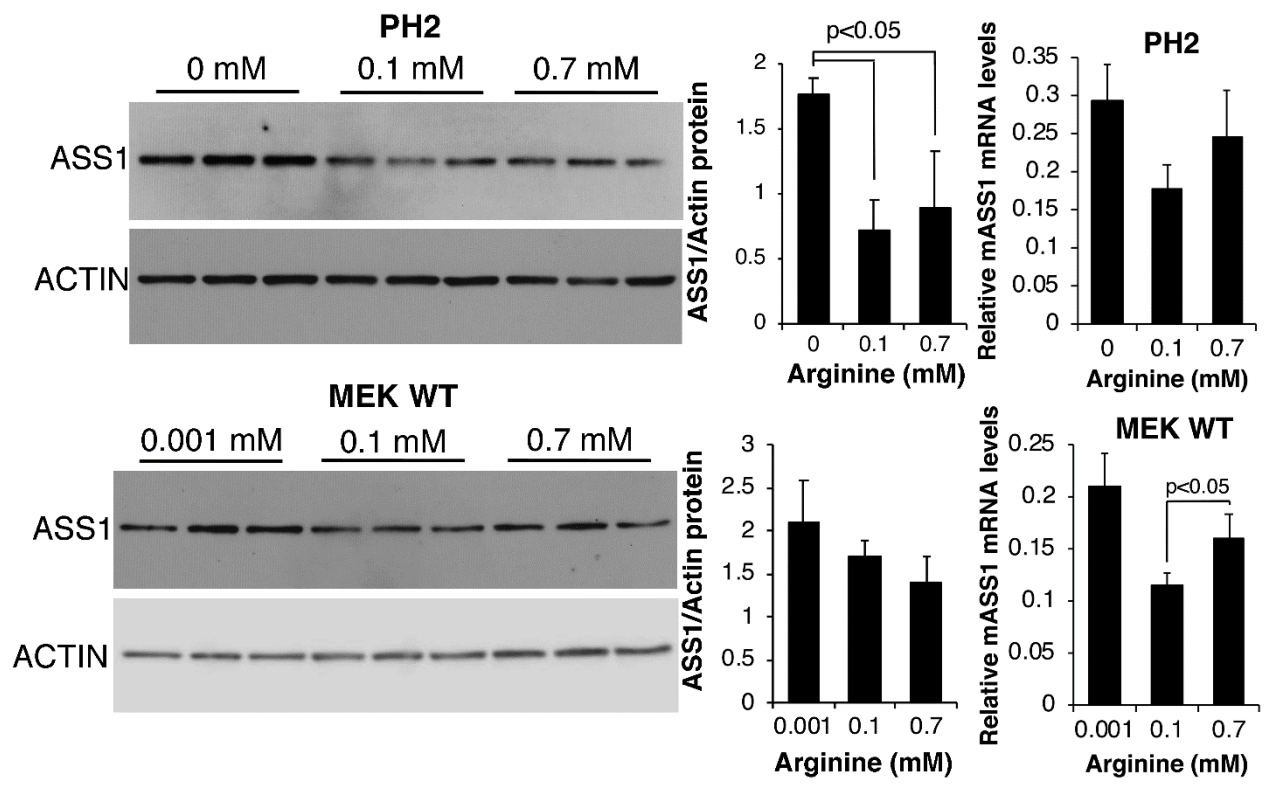

Fig. 6

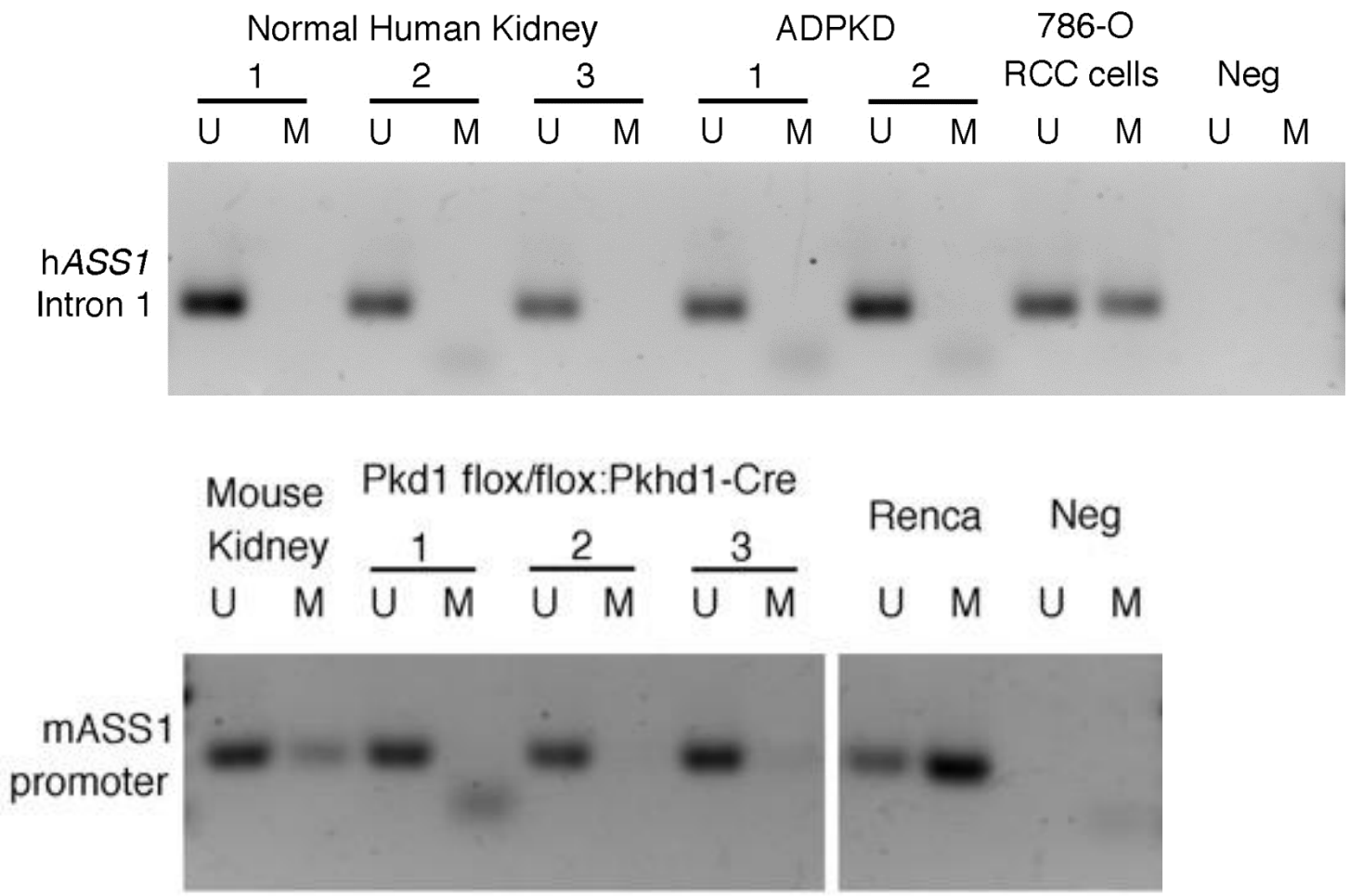

Fig. 7

a)

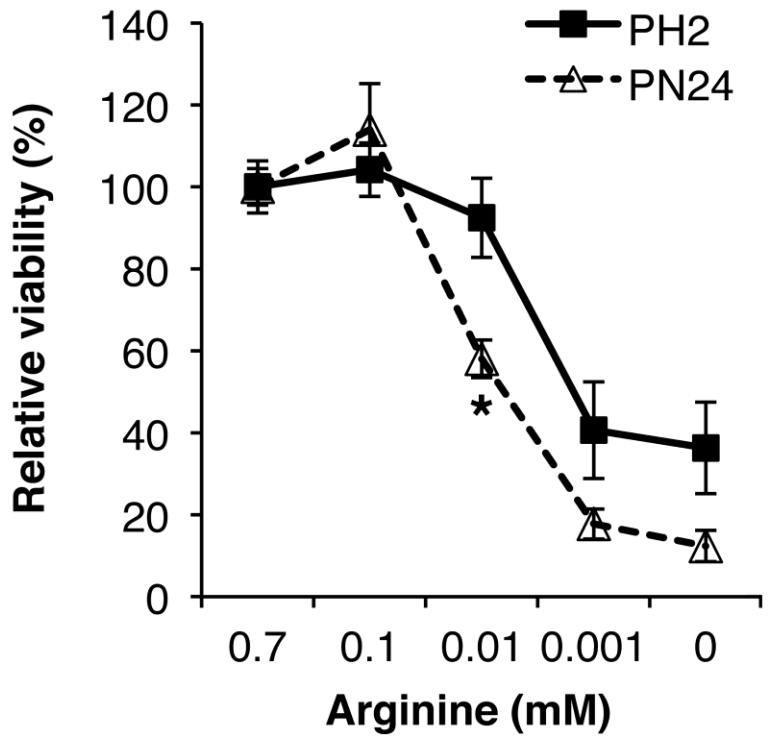

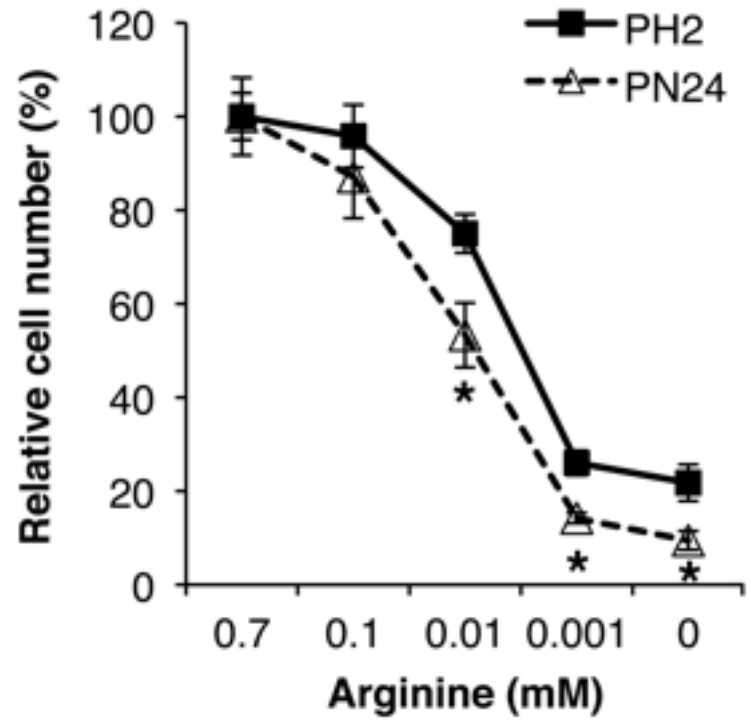

b)

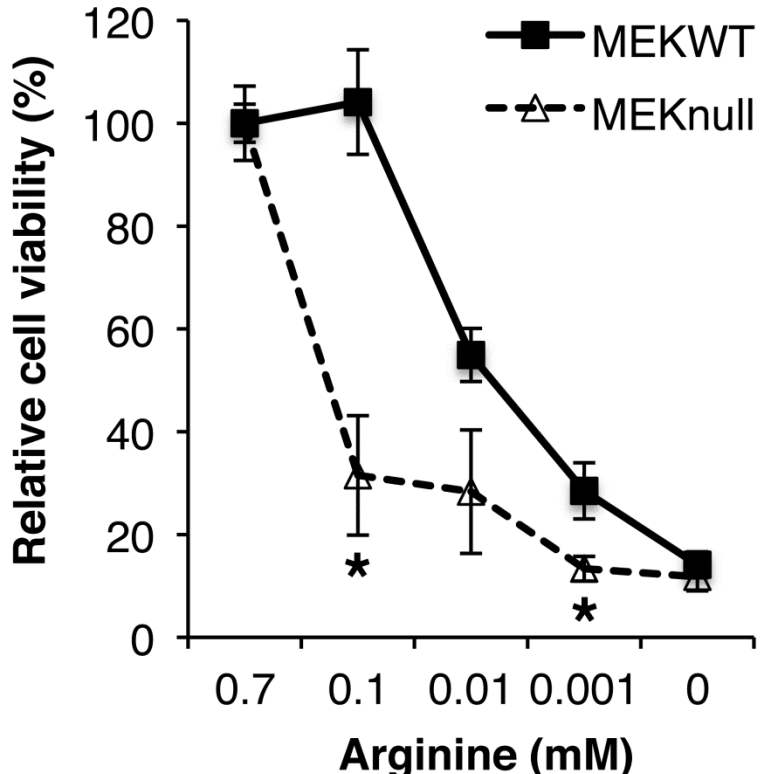

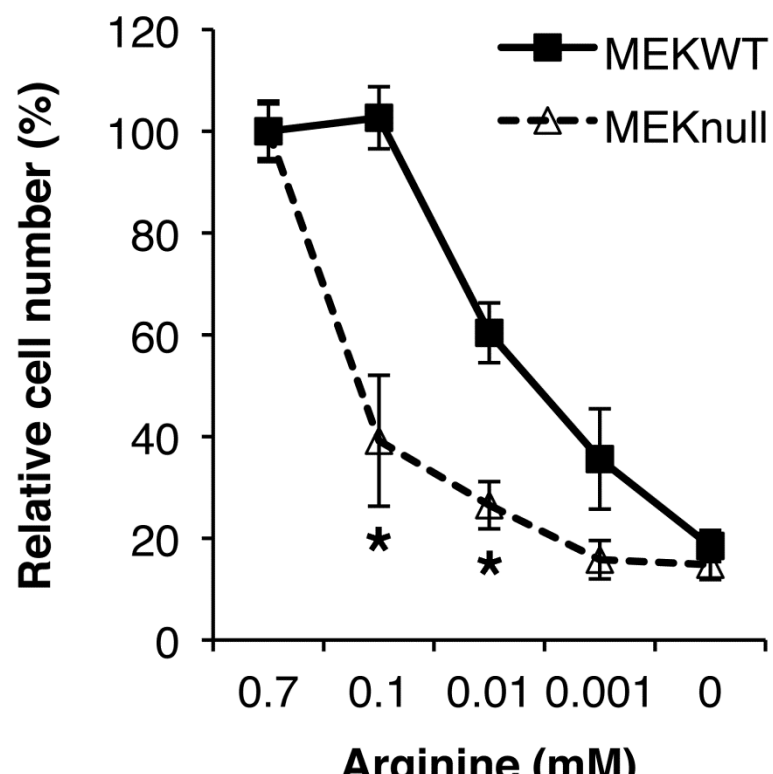

Fig. 8

PN24

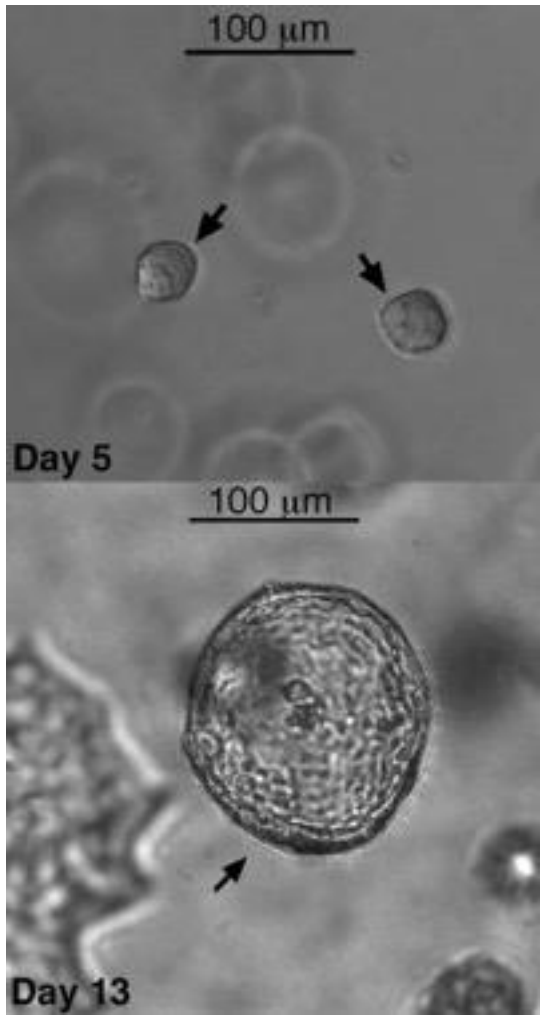

MEKnull

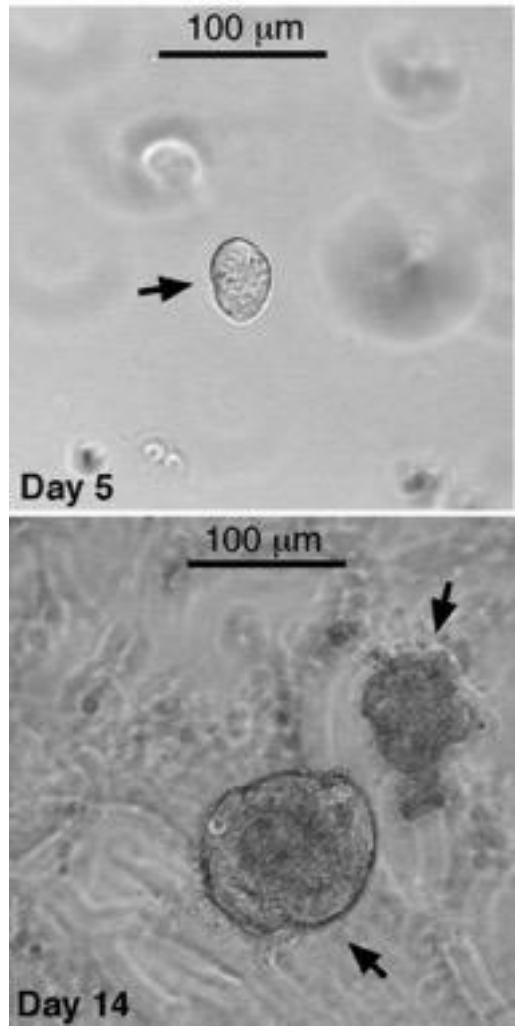

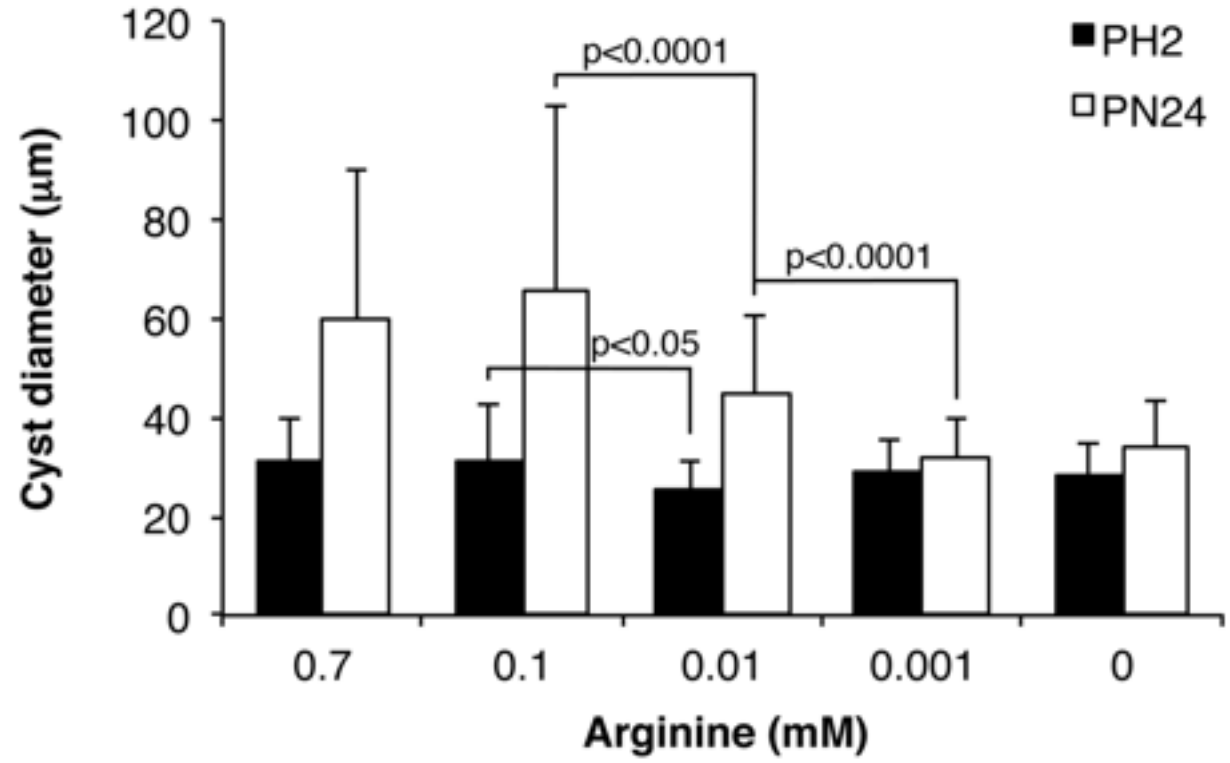

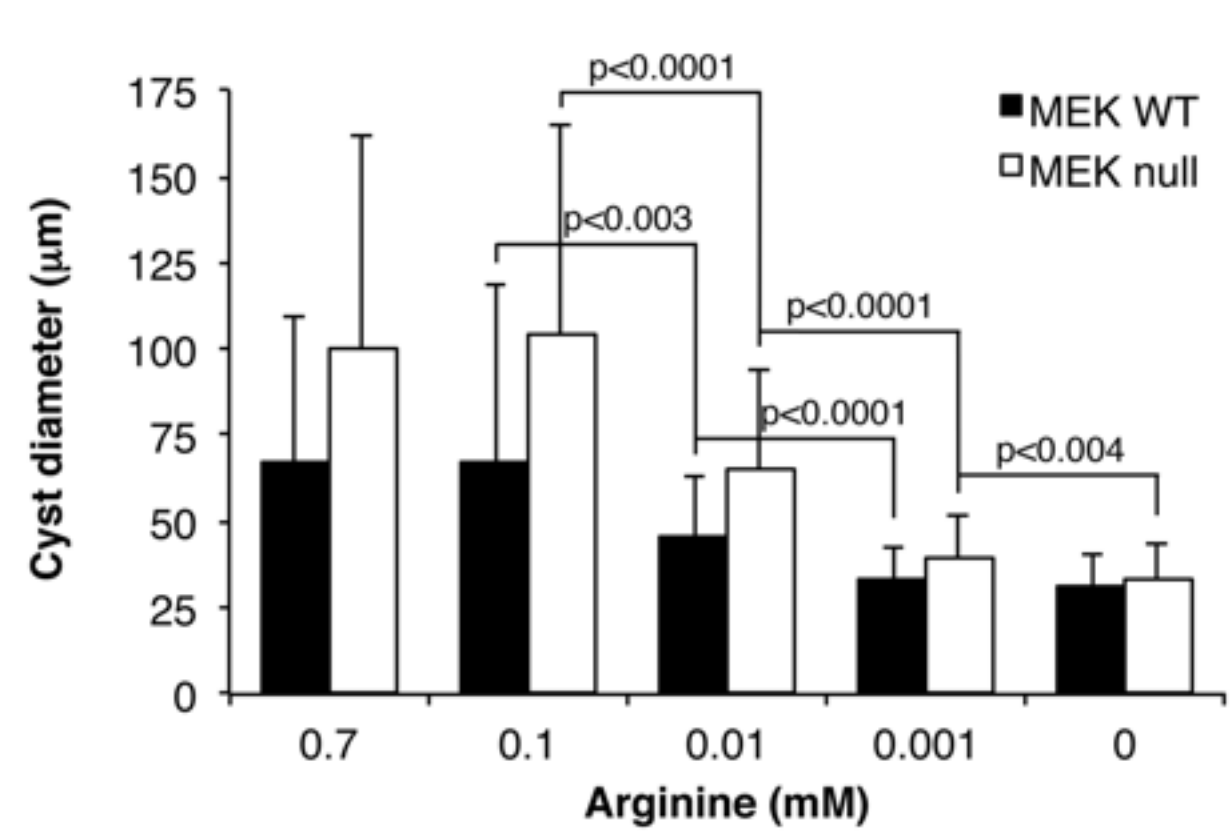

Fig. 9

a)

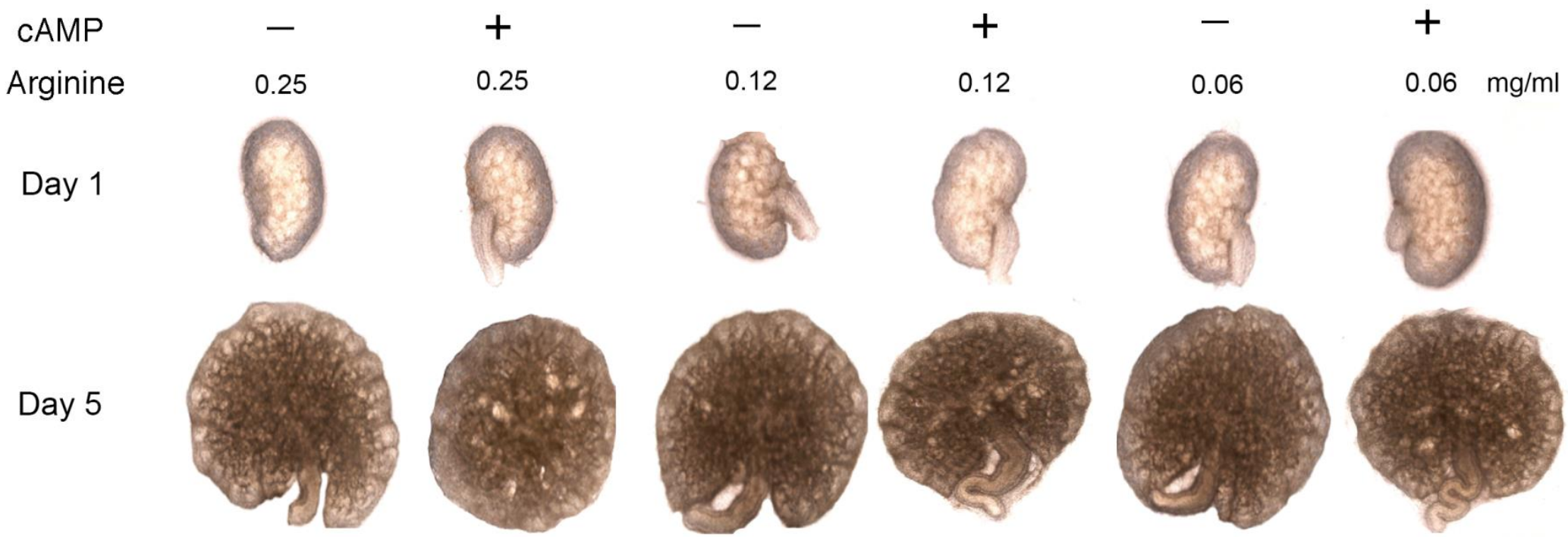

b)

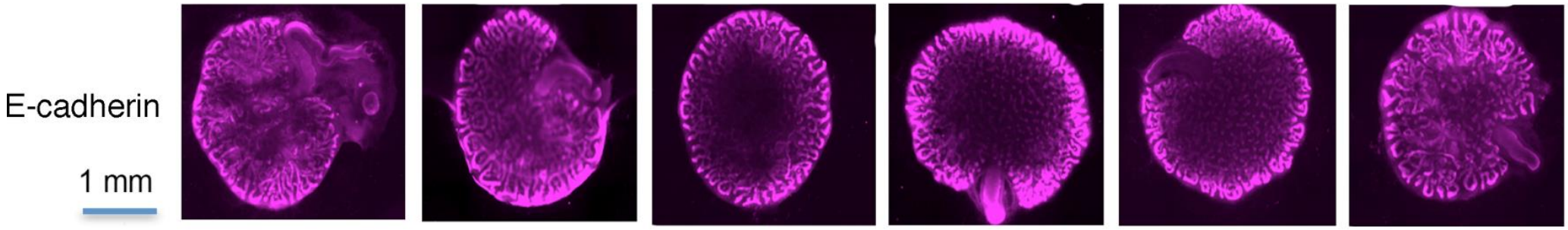

c)

1. 0.25 mg/ml Arg, no cAMP
2. 0.25 mg/ml Arg, cAMP
3. 0.12 mg/ml Arg, no cAMP
4. 0.12 mg/ml Arg, cAMP
5. 0.06 mg/ml Arg, no cAMP
6. 0.06 mg/ml Arg, cAMP

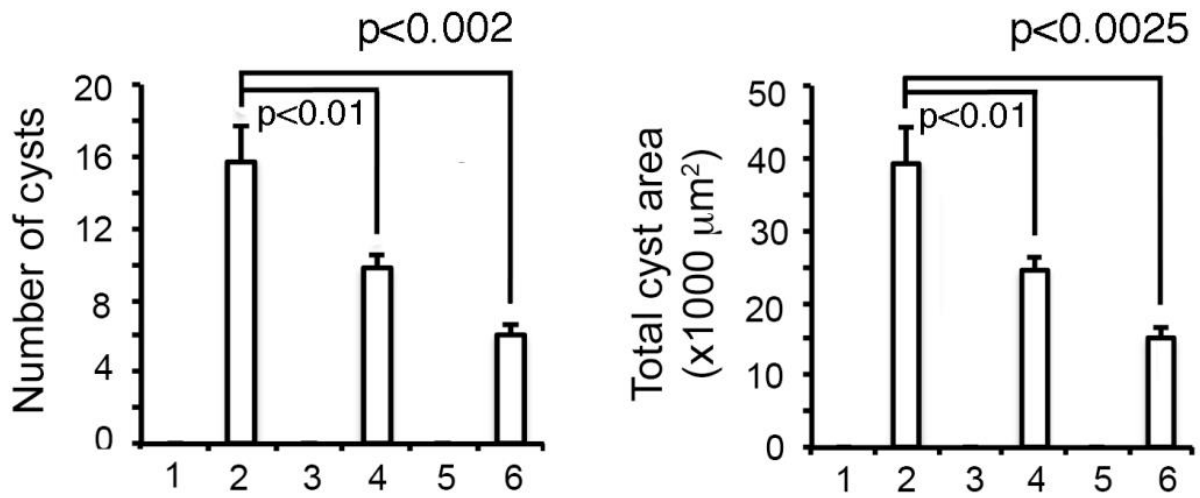

Fig. 10

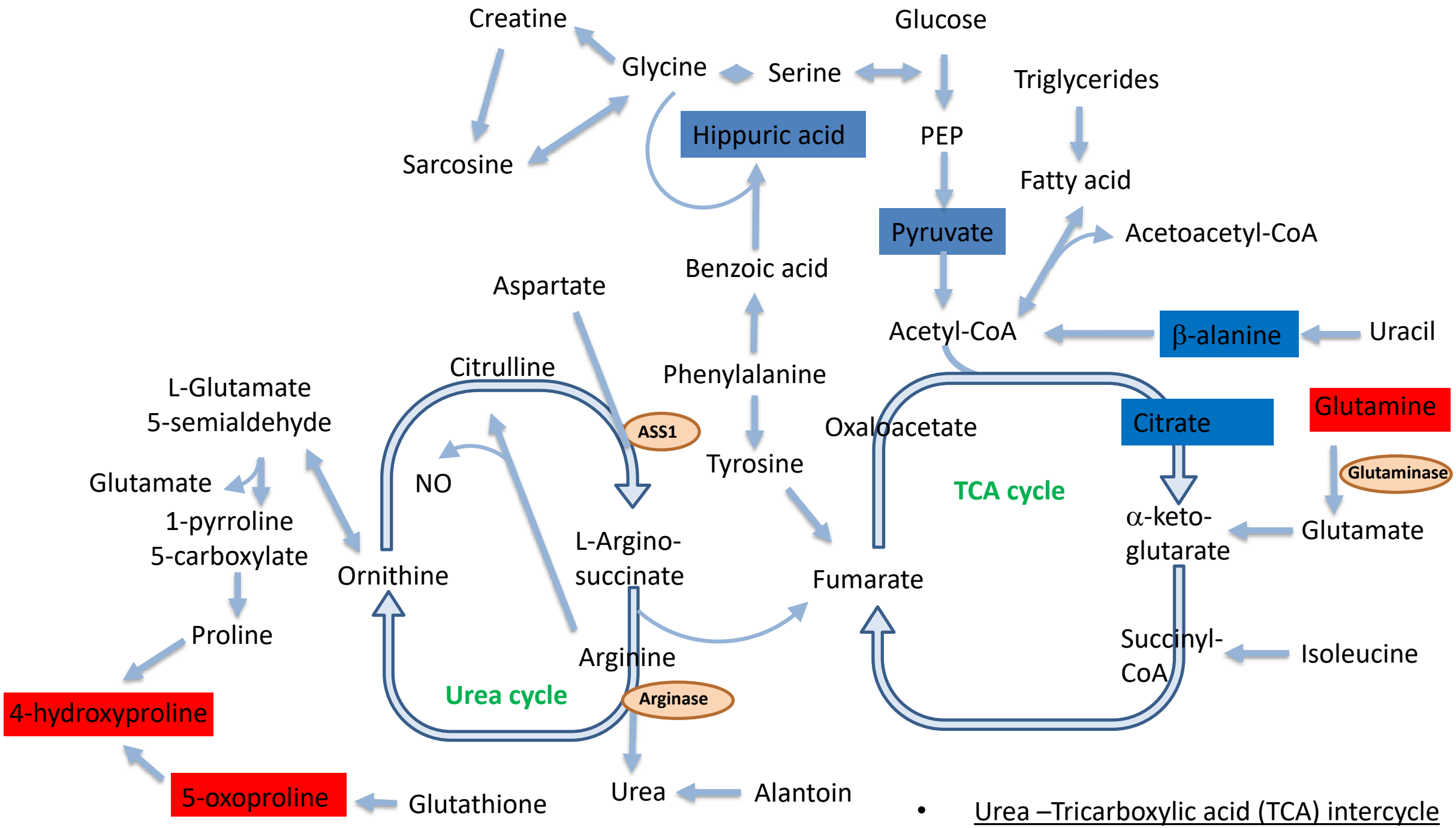

- Urea –Tricarboxylic acid (TCA) intercycle

Fig. 11

a)

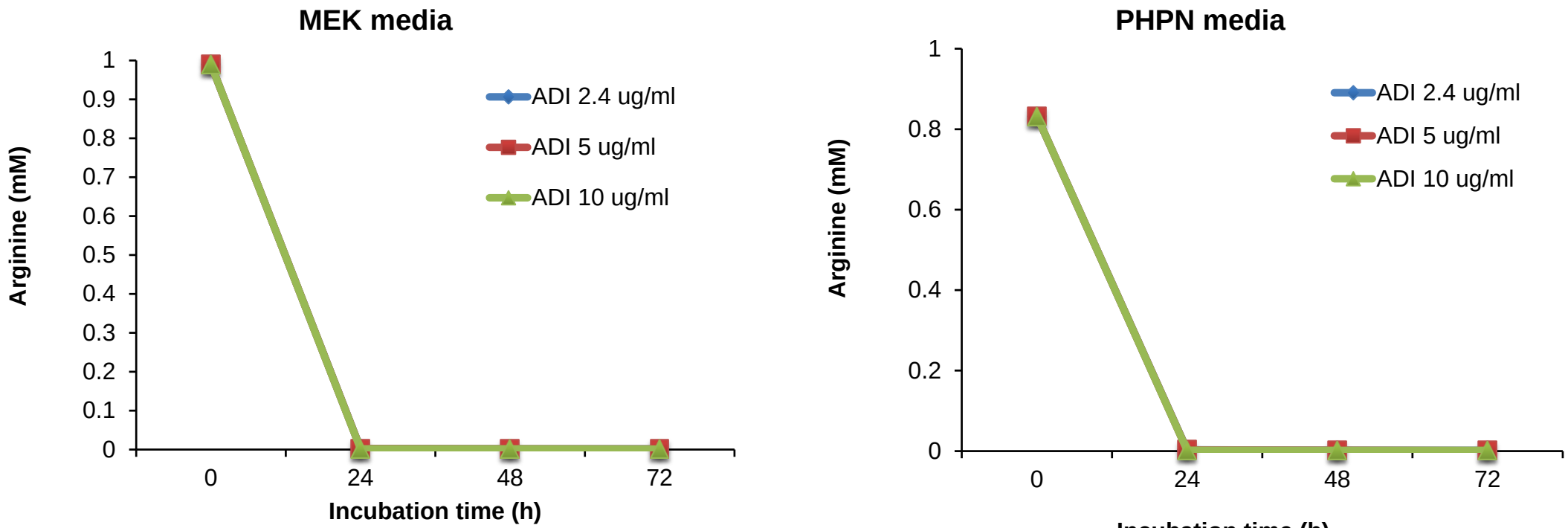

b)